NEUROSCIENCE

Opposite effects of stress on effortful motivation in high and low anxiety are mediated by CRHR1 in the VTA

Ioannis Zalachoras[1]*, Simone Astori[1]*, Mandy Meijer[1,2], Jocelyn Grosse[1], Olivia Zanoletti[1], Isabelle Guillot de Suduiraut[1], Jan M. Deussing[3], Carmen Sandi[1]*

Individuals frequently differ in their behavioral and cognitive responses to stress. However, whether motivation is differently affected by acute stress in different individuals remains to be established. By exploiting natural variation in trait anxiety in outbred Wistar rats, we show that acute stress facilitates effort-related motivation in low anxious animals, while dampening effort in high anxious ones. This model allowed us to address the mechanisms underlying acute stress–induced differences in motivated behavior. We show that CRHR1 expression levels in dopamine neurons of the ventral tegmental area (VTA)—a neuronal type implicated in the regulation of motivation—depend on animals' anxiety, and these differences in CRHR1 expression levels explain the divergent effects of stress on both effortful behavior and the functioning of mesolimbic DA neurons. These findings highlight CRHR1 in VTA DA neurons—whose levels vary with individuals' anxiety—as a switching mechanism determining whether acute stress facilitates or dampens motivation.

INTRODUCTION

Acute exposure to stressors activates a set of adaptive responses in the brain and peripheral physiological systems that orchestrate behavioral changes to cope with life threats (*1*, *2*). Despite its important motivational functions, the effect of acute stress in motivated behaviors is not clear. As opposed to the consensus that both chronic stress and stress-related psychopathologies are characterized by impaired motivation (*3*–*6*), findings on the motivational effects of acute stress are mixed (*7*–*11*). Although brief exposure to physical stressors tends to result in impaired motivation (*7*–*11*), some studies have reported improved performance (*12*) or no effects (*8*). Although differences in the characteristics of the stressors may contribute to this discrepancy, the existence of individual variability in the behavioral and cognitive responses to stress (*13*–*18*) may be key to understanding acute stress effects in motivated performance. This variability has been documented in other domains but remains unknown for motivation. For example, acute stress affects learning and memory (*19*, *20*), but only a subset of individuals shows detrimental performance under high stress, while others thrive (*18*, *21*). Similarly, stress affects social competitiveness (*22*), boosting dominant behaviors in some individuals while inducing subordination in others (*23*, *24*).

Anxiety, as a personality trait or temperamental predisposition, has been revealed as a key moderator of acute stress effects in both learning (*18*, *21*, *25*, *26*) and social behaviors (*23*, *24*). However, whether trait anxiety may explain variance in the modulation of motivated behaviors by stress is not known. Motivation—the process that facilitates overcoming the cost of an effortful action to achieve a desired outcome (*27*)—is crucial for both success and well-being (*28*, *29*). Therefore, identifying factors that account for individual differences in acute stress effects in motivated behavior could help both, revealing their neurobiological underpinnings and developing strategies to foster motivation under stress.

At the neurobiological level, a promising mechanism to mediate the interaction between anxiety and the neural substrates of motivated behavior is the regulation of the mesolimbic system by corticotropin-releasing hormone (CRH) actions through CRH receptor 1 (CRHR1) (*30*). On the one hand, the mesolimbic dopaminergic (DA) system, comprising DA projections from the ventral tegmental area (VTA) to the nucleus accumbens (NAc), is critical for motivation (*31*, *32*). On the other hand, CRH actions through CRHR1—the predominantly expressed CRH receptor in VTA DA neurons (*33*–*35*)—are central components of the physiological stress response and are involved in the regulation of anxiety phenotypes (*33*, *36*). In the VTA, acute stress has been shown to trigger CRH release (*10*) and CRHR1 to mediate stress-induced impairments in motivated behaviors (*9*, *11*). Given that mice with genetic deletion of *Crhr1* in DA—but not gamma-Aminobutyric acid (GABA)-ergic—neurons show increased anxiety (*37*), we hypothesize here a role for CRHR1 in DA neurons on anxiety-dependent effects of stress in motivated behaviors.

Here, we investigate anxiety-related differences in motivated behaviors under stress and their underlying mechanisms. We use outbred Wistar rats, a natural model of variation in trait anxiety (*24*, *38*), and assess effort to obtain rewards in an operant task under a progressive ratio schedule following acute stress exposure. By combining behavioral, genetic, electrophysiological, histochemical, and molecular analyses along with pharmacological and genetic manipulations, we show opposite motivational effects of stress depending on individuals' anxiety and implicate differences in the expression levels of CRHR1 in the VTA DA neurons in these effects.

RESULTS

Acute stress has opposite effects in motivated behavior in low anxious and high anxious rats

First, we classified animals as either low (LA) or high (HA) anxious according to their performance in the elevated plus maze (EPM; Fig. 1A) and following established criteria (*24*). Then, LA and HA rats were trained in an operant conditioning task under a fixed ratio

[1]Laboratory of Behavioral Genetics, Brain Mind Institute, École Polytechnique Fédérale de Lausanne, Lausanne, Switzerland. [2]Department of Human Genetics, Donders Institute for Brain, Cognition and Behaviour, Radboud University Medical Center, Nijmegen, Netherlands. [3]Max Planck Institute of Psychiatry/Molecular Neurogenetics, Munich, Germany.
*Corresponding author. Email: carmen.sandi@epfl.ch (C.S.); izalacho@hotmail.com (I.Z.); simone.astori@epfl.ch (S.A.)

1 (FR1) schedule to obtain palatable food rewards in which both groups showed similar performance [two-way repeated-measures analysis of variance (ANOVA) revealed a nonsignificant session × anxiety interaction ($F_{5,125}$ = 1.519, P = 0.189); fig. S1B]. However, when subsequently tested in a progressive ratio schedule (PR test; fig. S1C), either under basal conditions or following acute stress exposure [i.e., exposure to an elevated platform (EP) during 15 min; Fig. 1B], we found a key interaction between stress and anxiety trait (Fig. 1C). We confirmed that exposure to the EP elicited a robust stress response regardless of anxiety, as indicated by marked increases in plasma corticosterone levels that did not correlate with animals' basal anxiety (fig. S1A). Whereas performance did not differ between the two anxiety groups under basal conditions (LA-ctr and HA-ctr), stress increased motivated behaviors in LA rats (LA-stress) but had the opposite, detrimental effect in HA (HA-stress) rats. Thus, LA-stress and HA-stress differed from their respective control groups for breakpoint [two-way ANOVA revealed a significant stress × anxiety interaction ($F_{1,36}$ = 15.46, P = 0.0004); Fig. 1C], number of correct nosepokes [two-way ANOVA revealed a significant stress × anxiety interaction ($F_{1,36}$ = 12.35, P = 0.001); Fig. 1D], and number of obtained rewards [two-way ANOVA revealed a significant stress × anxiety interaction ($F_{1,36}$ = 12.42, P = 0.001); Fig. 1E]. In addition, LA-stress rats showed superior performance than HA-stress for all those parameters (Fig. 1, D and E). Although stress led to fewer incorrect nosepokes (in the inactive port; fig. S1D), there were no group differences in the number of correct nosepokes during the timeout period (fig. S1E). Moreover, there were no group differences in the consumption of 20 pellets in a free access test (i.e., the same type of pellets and in an amount equivalent to the maximal number they could obtain as rewards in the PR test; fig. S1F), suggesting that the observed performance differences in the PR test are not due to stress-induced changes in the perceived palatability of the pellets or on animals' motivation to eat, but rather related to their motivation to exert effort to obtain the reward.

To corroborate these findings, we performed another experiment with a new cohort of animals but, this time, instead of using different rats for each condition (control or stress) as above, we tested the same animals in the PR test first under control and then under stress conditions. Again, performance of LA and HA rats was equivalent under basal conditions, but diverged following acute stress exposure. LA rats significantly improved their motivated behavior after stress and showed better performance than HA rats for breakpoint [two-way ANOVA revealed a significant stress × anxiety interaction ($F_{1,19}$ = 9.949, P = 0.0052); fig. S1G] for correct nosepokes [two-way ANOVA revealed a significant stress × anxiety interaction ($F_{1,19}$ = 25.57, P < 0.0001); fig. S1H] and number of obtained rewards [two-way ANOVA revealed a significant stress × anxiety interaction ($F_{1,19}$ = 13.04, P = 0.0019); fig. S1I].

Crhr1 common variant is associated with anxiety

To investigate whether the CRH system is a potential substrate for the behavioral differences observed above, we then asked whether genetic variants in intron 1 of *Crhr1* are associated with anxious behavior. In total, 26 HA, 32 intermediate anxious (IA), and 35 LA rats were genotyped (Fig. 2), and variation in a known single-nucleotide polymorphism (SNP; rs106600307, chr10:92191940) was identified. Haplotype distribution was associated with anxious behavior measured by the EPM (Kruskal-Wallis χ^2 = 6.2139, df = 2, P = 0.04474) in an overdominant fashion (Fig. 2A). Heterozygote animals were less anxious than homozygote animals for either the reference (G/G) or the alternative (A/A) allele (Wilcoxon rank sum test, W = 1397.5, P = 0.01309), possibly caused by altered *Crhr1* expression and activity levels (Fig. 2B). Moreover, our analyses revealed that a higher proportion of LA rats are heterozygous for this SNP, whereas a higher proportion of HA rats are homozygous, confirming that the heterozygous SNP is associated with lower anxiety in Wistar rats (Fig. 2C).

LA rats have higher CRHR1 expression in VTA DA neurons than HA rats

To verify that expression patterns of CRHR1 are implicated in anxious behavior and motivation, we then asked whether LA and HA rats display a differential CRHR1 expression in the VTA. Given that CRHR1 deletion in different cell types induces opposing effects on anxiety (i.e., anxiogenic in DAergic neurons, while anxiolytic in GABAergic neurons) (*37*), we performed a cell type–specific quantitative analysis of *Crhr1* mRNA and protein levels. RNAscope fluorescence in situ

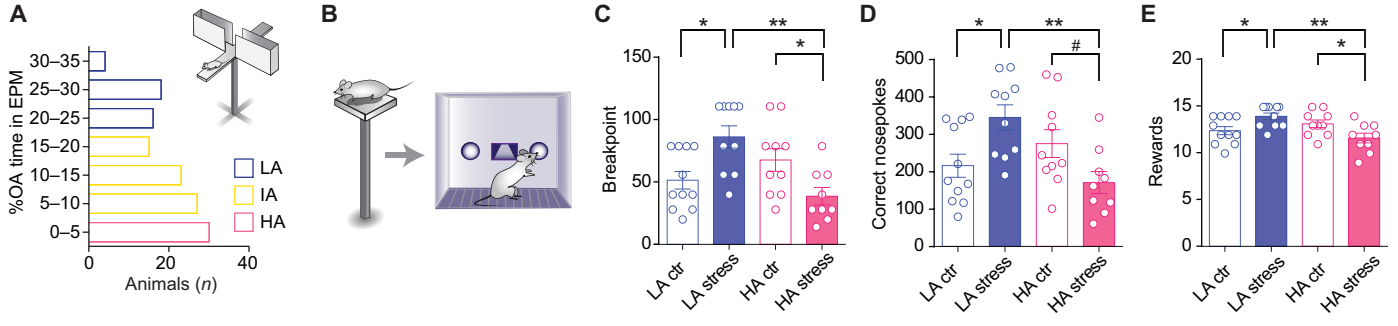

Fig. 1. Effects of acute exposure to stress on PR test performance. (**A**) All rats were phenotyped for trait anxiety in the EPM before the beginning of experiments. Bar graphs represent the distribution of the time spent in the open arms (%OA) in a representative batch of 130 rats. (**B**) Scheme describing the experiment probing the effects of acute stress exposure on PR test performance of LA and HA rats. (**C**) Stress exposure resulted in a higher breakpoint in LA rats compared to HA rats. Two-way ANOVA revealed a significant stress × anxiety interaction ($F_{1,36}$ = 15.46, P = 0.0004), but no significant effects of anxiety or stress ($F_{1,36}$ = 3.736, P = 0.061 and $F_{1,30}$ = 0.1244, P = 0.726, respectively, n = 9 to 11 per group). (**D**) LA rats exposed to stress performed significantly more nosepokes than HA rats exposed to stress. Two-way ANOVA revealed a significant stress × anxiety interaction ($F_{1,36}$ = 12.35, P = 0.001), but no significant effects of anxiety or stress ($F_{1,36}$ = 3.010, P = 0.091 and $F_{1,36}$ = 0.141, P = 0.71, respectively, n = 9 to 11 per group). (**E**) LA rats exposed to stress acquired more rewards than HA rats exposed to stress. Two-way ANOVA revealed a significant stress × anxiety interaction ($F_{1,36}$ = 12.42, P = 0.001), but no significant effects of anxiety or stress ($F_{1,36}$ = 3.304, P = 0.077 and $F_{1,36}$ = 0.0001, P = 0.99, respectively, n = 9 to 11 per group). Asterisks denote significant differences in the respective post hoc tests (**P < 0.01, *P < 0.05, and $^{\#}P$ < 0.1).

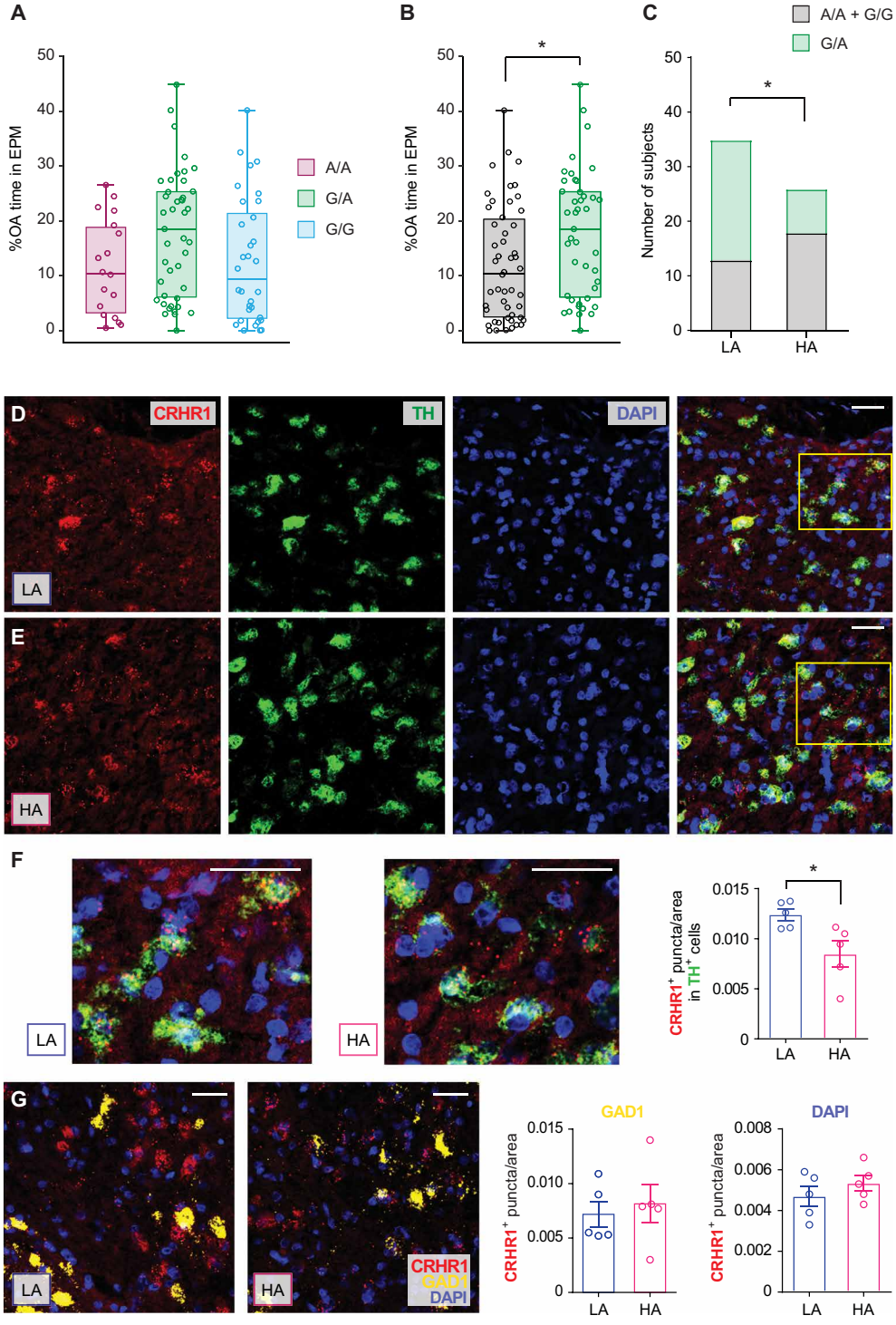

Fig. 2. Trait anxiety is associated with a *Crhr1* common variant and with different CRHR1 expression in VTA DA neurons. (**A** to **C**) All rats ($n = 26$ HA, $n = 32$ IA, and $n = 35$ LA) were genotyped for SNP on rs106600307 located on chr10:92191940. (A) Allele pair distribution is associated with time spent in the open arms in the EPM (Kruskal-Wallis $\chi^2 = 6.2139$, df = 2, $P = 0.04474$). (B) Heterozygous rats spent significantly more time in the open arms of the EPM compared to homozygous rats (Wilcoxon rank sum test, $W = 1397.5$, $P = 0.01309$). Bars represent the percentage of time spent in the open arms (%OA) for the different allele pairs. (C) A significantly higher proportion of LA rats than HA rats are heterozygous for the *Crhr1* SNP (χ^2 test$_{6.146,1}$, $P = 0.0132$). (**D** to **F**) CRHR1 expression in DA cells in the VTA was probed with RNAscope. Expression of CRHR1 mRNA (red) in TH$^+$ cells (green), along with nuclear staining with DAPI (blue) and merged image in the VTA of LA (D) and HA (E) rats. (F) Left: Higher magnification images of the marked area of panels in (D) and (E) in LA and HA rats. Right: LA rats had higher CRHR1 mRNA expression in DA neurons in the VTA than HA rats (Mann-Whitney test, $U = 2.000$, $P = 0.032$). (**G**) Left: CRHR1 expression in GABAergic cells in the VTA. Merged images of expression of CRHR1 mRNA (red) in GAD1$^+$ cells (magenta), along with nuclear staining with DAPI (blue) in LA and HA rats. Right: CRHR1 mRNA expression was not different between LA and HA rats in GABAergic neurons (Mann-Whitney test, $U = 11.00$, $P = 0.816$) and when quantified in all nuclei (Mann-Whitney test, $U = 8.500$, $P = 0.46$). *$P < 0.05$. Scale bars, 100 μm.

hybridization analysis in the VTA revealed a significantly higher *Crhr1* expression in DA [tyrosine hydroxylase–positive (TH^+)] neurons of LA rats than in those of HA rats (Fig. 2, D to F), but no differences in *Crhr1* expression in GABAergic ($GAD1^+$) neurons or when counting expression in all cell nuclei [stained with 4′,6-diamidino-2-phenylindole (DAPI); Fig. 2G]. To corroborate our findings in DA neurons, we performed a double immunofluorescence staining for CRHR1 and TH in the VTA. CRHR1 immunofluorescence in DA neurons in the VTA of LA rats was higher than in that of HA rats (fig. S1, J to L), indicating that the observed anxiety-related differences in CRHR1 expression in VTA DA neurons are also reflected at the protein level. Together, these data reveal that trait anxiety differences are coupled to differences in CRHR1 expression in VTA DA neurons, pointing at CRHR1 in VTA DA neurons as a potential substrate for the anxiety-dependent divergent effects of stress in motivated behavior.

Intra-VTA CRH treatment mimics the effects of stress on motivated behavior in LA and HA rats

CRH actions in the VTA can mimic detrimental effects of acute stress in motivated behavior (*9*, *11*). Given our findings on anxiety-dependent differential expression of VTA CRHR1 levels, we hypothesized that intra-VTA CRH effects may differ depending on animals' anxiety trait, mimicking the divergent motivational effects induced by acute stress in LA and HA rats. To test this hypothesis, following cannulation and then FR1 training (there were no group differences in performance; fig. S2A), LA and HA rats were bilaterally infused with vehicle (LA-Veh, HA-Veh) or CRH (LA-CRH, HA-CRH) and then tested in the PR test (Fig. 3A). Mirroring the acute stress results, CRH infusion improved performance in LA rats (LA-CRH versus LA-Veh) but impaired performance in HA rats (HA-CRH versus HA-Veh), and LA-CRH showed superior performance than HA-CRH [two-way ANOVA revealed a significant treatment × anxiety interaction ($F_{1,26} = 21.50$, $P < 0.0001$), for breakpoint, Fig. 3B; two-way ANOVA revealed a significant treatment × anxiety interaction ($F_{1,26} = 17.93$, $P = 0.0003$), for correct nosepokes, Fig. 3C; two-way ANOVA revealed a significant treatment × anxiety interaction ($F_{1,26} = 21.50$, $P < 0.0001$), for obtained rewards, Fig. 3D]. No differences were observed in training performance between LA and HA rats following cannulation (fig. S2A), in incorrect nosepokes during PR (fig. S2B), in the correct nosepokes during the timeout period (fig. S2C), or in the total number of pellets eaten when given 15-min free access to them (fig. S2D) regardless of treatment or anxiety group. Furthermore, in a new cohort of animals, microdialysis experiments (fig. S2E) indicated that while LA-Veh and HA-Veh showed similar levels of DA and DOPAC (3,4-dihydroxyphenylacetic acid) in the NAc (fig. S2F), LA-CRH rats displayed higher levels of both DA and DOPAC (fig. S2G). This confirms a differential responsiveness of the mesolimbic DAergic system to VTA CRH actions depending on trait anxiety.

Differential action of CRH on VTA DA firing in LA and HA rats

Given our findings here that (i) CRHR1 levels in DA VTA neurons differ between LA and HA rats and (ii) intra-VTA CRH actions exert opposite effects in LA and HA rats' motivated behavior, we postulated that the substrate for the latter may rely on a differential responsiveness of VTA DA neurons to CRH in the two anxiety groups. To test this possibility, we conducted ex vivo patch clamp recordings from DA neurons—identified based on their electrophysiological signature (see Materials and Methods and fig. S3, A to C). DA VTA neurons from LA and HA rats displayed comparable intrinsic excitability, with overlapping frequency-current relationships when firing was elicited by somatic current injections, as well as comparable rheobase and firing threshold (fig. S3, E to G), and hyperpolarization-activated cyclic nucleotide–gated (HCN) channel-induced I_h currents (fig. S3, H to J). To examine the acute effects of CRH on spontaneous DA VTA neuron firing, we bath-applied CRH (500 nM), which in LA rats induced a reversible increase that was prevented by the CRHR1 antagonist CP-154526 (3 μM). Notably, in HA rats, the facilitating effect of CRH on DA VTA neuron spiking was blunted (>4-fold smaller than in LA rats; Fig. 4A). The dose-response curves confirmed a significant difference between LA and HA rats throughout the submillimolar range (Fig. 4B). Recordings of spontaneous cell firing ex vivo revealed that DA neurons from LA rats were generally silent under basal conditions, whereas DA neurons from HA rats

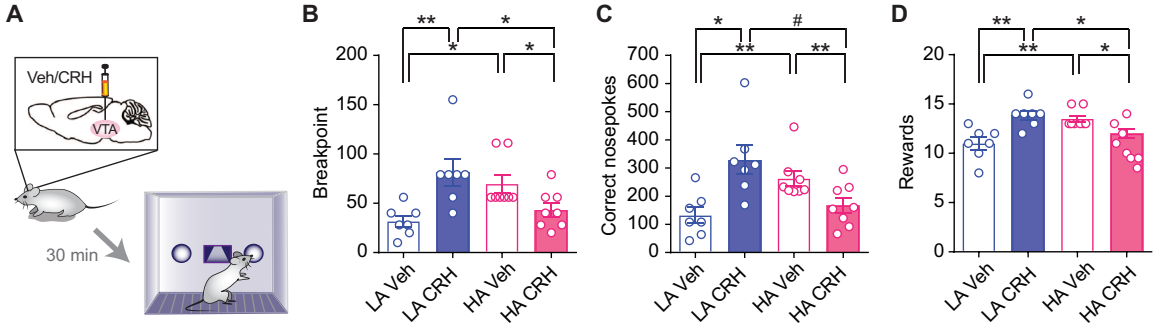

Fig. 3. Effects of intra-VTA CRH administration on PR test performance. (**A**) Scheme describing the experiment probing the effects of intra-VTA CRH administration on PR test performance of LA and HA rats. (**B**) Vehicle-treated HA rats had a higher breakpoint compared to vehicle-treated LA rats. Intra-VTA CRH treatment in LA rats resulted in a higher breakpoint compared to CRH-treated HA rats. Two-way ANOVA revealed a significant treatment × anxiety interaction ($F_{1,26} = 17.01$, $P = 0.0003$), but no significant effects of anxiety or treatment ($F_{1,26} = 0.0005$, $P = 0.98$ and $F_{1,26} = 1.560$, $P = 0.223$, respectively, $n = 7$ to 8 per group). (**C**) Intra-VTA CRH administration in LA rats resulted in higher number of correct nosepokes performed compared to CRH-treated HA rats. Two-way ANOVA revealed a significant treatment × anxiety interaction ($F_{1,26} = 17.93$, $P = 0.0003$), but no significant effects of anxiety or treatment ($F_{1,26} = 0.204$, $P = 0.65$ and $F_{1,26} = 2.170$, $P = 0.153$, respectively, $n = 7$ to 8 per group). (**D**) Vehicle-treated HA rats acquired a higher number of rewards compared to vehicle-treated LA rats. However, intra-VTA CRH treatment in LA rats resulted in a higher number of acquired rewards compared to CRH-treated HA rats. Two-way ANOVA revealed a significant treatment × anxiety interaction ($F_{1,26} = 21.50$, $P < 0.0001$), but no significant effects of anxiety or treatment ($F_{1,26} = 0.468$, $P = 0.50$ and $F_{1,26} = 2.086$, $P = 0.161$, respectively, $n = 7$ to 8 per group). Asterisks denote significant differences between anxiety groups at respective time points (**$P < 0.01$, *$P < 0.05$ and $^{\#}P < 0.1$).

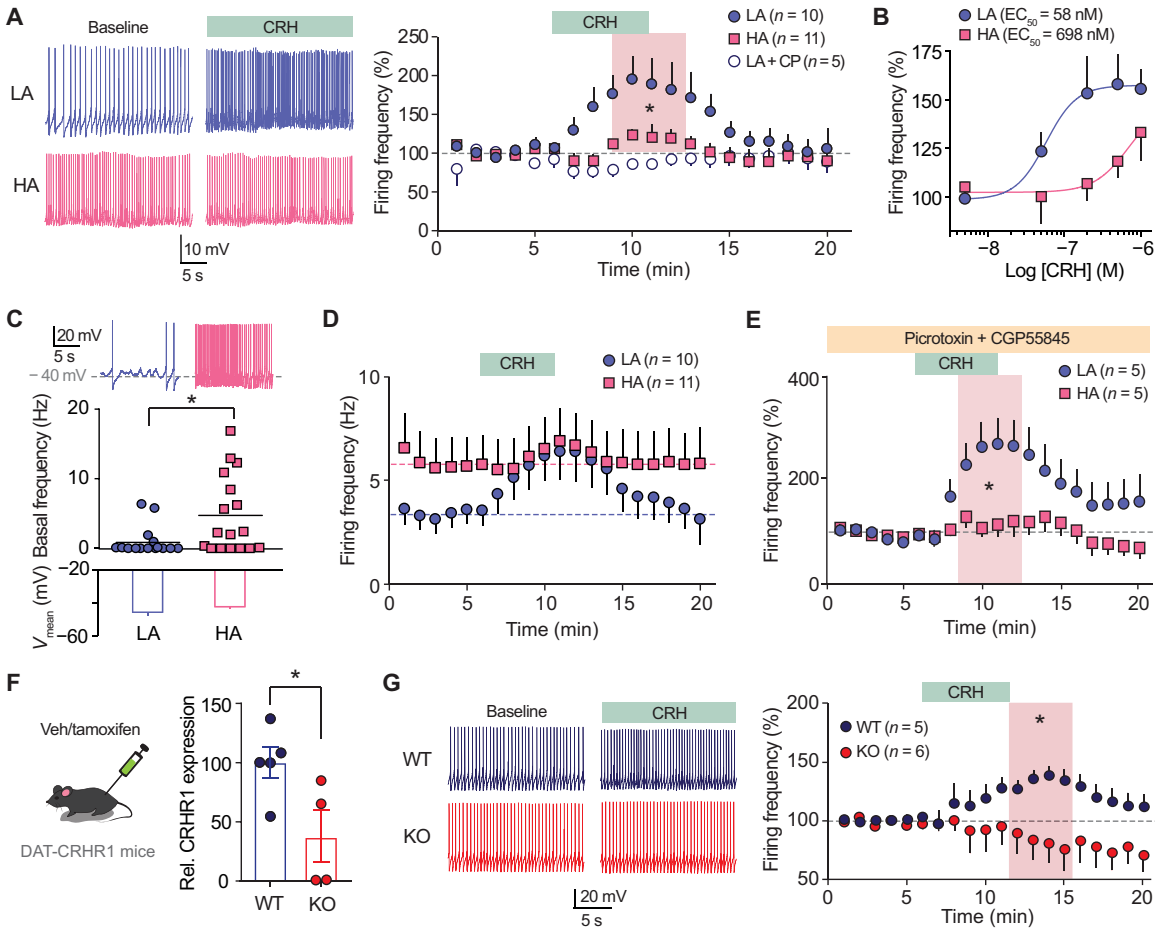

Fig. 4. Effects of CRH on VTA DA neuron firing. (**A**) Bath application of CRH (500 nM) induced a reversible increase in DA VTA cell firing, more pronounced in LA rats, and abrogated in LA rats by CRHR1 antagonist CP-154526 (3 μM) (Kruskal-Wallis: 14.16, $P = 0.0008$, Dunn's post hoc: LA versus HA, $P = 0.04$; LA versus LA + CP, $P = 0.0002$; $n = 10$-11-5). Color-coded representative traces recorded before and during CRH application on the left. (**B**) Dose-response curves for submillimolar concentrations of CRH on DA VTA cell firing in LA and HA rats (fit comparison: $F_{4,49} = 3.726$, $P = 0.010$, $n = 4, 4, 6, 9$, and 5 for LA and $n = 3, 4, 4, 11$, and 7 for HA for increasing concentration values). (**C**) Spontaneous firing frequency recorded in DA VTA neurons with no current injection appeared reduced in LA rats (Mann-Whitney: $U = 66.5$, $P = 0.0163$, $n = 15$ to 17). Representative voltage traces at the top. (**D**) Data presented in (A) are here represented as absolute firing values. (**E**) The anxiety-related differential effect of CRH on DA VTA cells persisted in the presence of the $GABA_AR$ blocker picrotoxin (100 μM) and the $GABA_BR$ blocker CGP55845 (2 μM) (Mann-Whitney test comparing mean values in the shaded area, $U = 2.0$, $P = 0.0317$, $n = 5$). (**F**) Quantification of CRHR1 expression levels in VTA tissue from WT and DAT-CRHR1 KO mice (two-tailed t test, $t_7 = 2.551$, $P = 0.0381$). (**G**) Bath application of CRH (500 nM) induced a reversible increase in cell firing in WT mice, which was absent in DAT-CRHR1 KO mice (Mann-Whitney test comparing mean values in the shaded area, $U = 2$, $P = 0.0317$, $n = 5$ to 6). Color-coded representative traces recorded before and during CRH application on the left. *$P < 0.05$.

exhibited higher spiking rates (Fig. 4C). Accordingly, the effect of CRH on the absolute values of firing frequency revealed that the nearly silent activity observed in LA cells under baseline conditions switched to high firing levels upon CRHR1 activation, reaching a maximal firing rate similar to the one recorded in HA rats upon basal and CRH conditions (Fig. 4D). Thus, as opposed to the blunted effects observed in HA rats, in LA rats CRH leads DA VTA neurons to change dynamically from low to high firing rate. On its turn, this is supposed to lead to a pronounced increase in DA release in VTA targets (*39*), consistent with the higher NAc DA levels found in LA rats, but not HA rats, after CRH infusion in the VTA (fig. S2, F and G).

VTA interneurons express presynaptic CRHR1 that can potentiate GABA release onto DA neurons (*40*). We thus tested whether the differential outcome of acute CRH application on DA VTA cell firing could be brought about by a differential modulation of the GABAergic tone in LA and HA rats. However, when inhibitory transmission was blocked, the different responsiveness in firing frequency to CRH in the two anxiety groups was preserved (Fig. 4E). Moreover, non-DA VTA neurons did not change their spontaneous firing when exposed to CRH (fig. S3D). We further verified that CRHR1 expressed in DA VTA neurons is necessary to induce the change in cell firing by using a tamoxifen-inducible DAT-CRHR1 mouse model (*41*), in which CRHR1 knockout (KO) was selectively induced in DA cells. CRHR1 KO in the VTA was verified using quantitative polymerase chain reaction (qPCR; Fig. 4F). Bath application of CRH (500 nM) led to a reversible increase in firing in wild-type (WT) mice, which was completely absent in DAT-CRHR1-KO mice (Fig. 4G). Collectively, these data indicate that CRH impinges primarily on intrinsic excitability mechanisms of DA VTA neurons, with a divergent responsiveness in LA and HA rats that is consistent with their differential expression of CRHR1 in VTA DA neurons.

Lower motivated performance under stress by down-regulation of CRHR1 expression in the VTA

From the previous results, we hypothesized that down-regulation of CRHR1 expression in the VTA would block the effects of stress on PR performance. To investigate the causal involvement of CRHR1 in the mediation of stress effects on motivated behavior, we undertook two approaches. First, we induced a down-regulation of CRHR1 expression in the VTA of LA rats using an antisense oligonucleotide (AON; Fig. 5, A and B), previously shown to be effective (*42*). Rats cannulated in the VTA were first trained in an FR1 schedule and

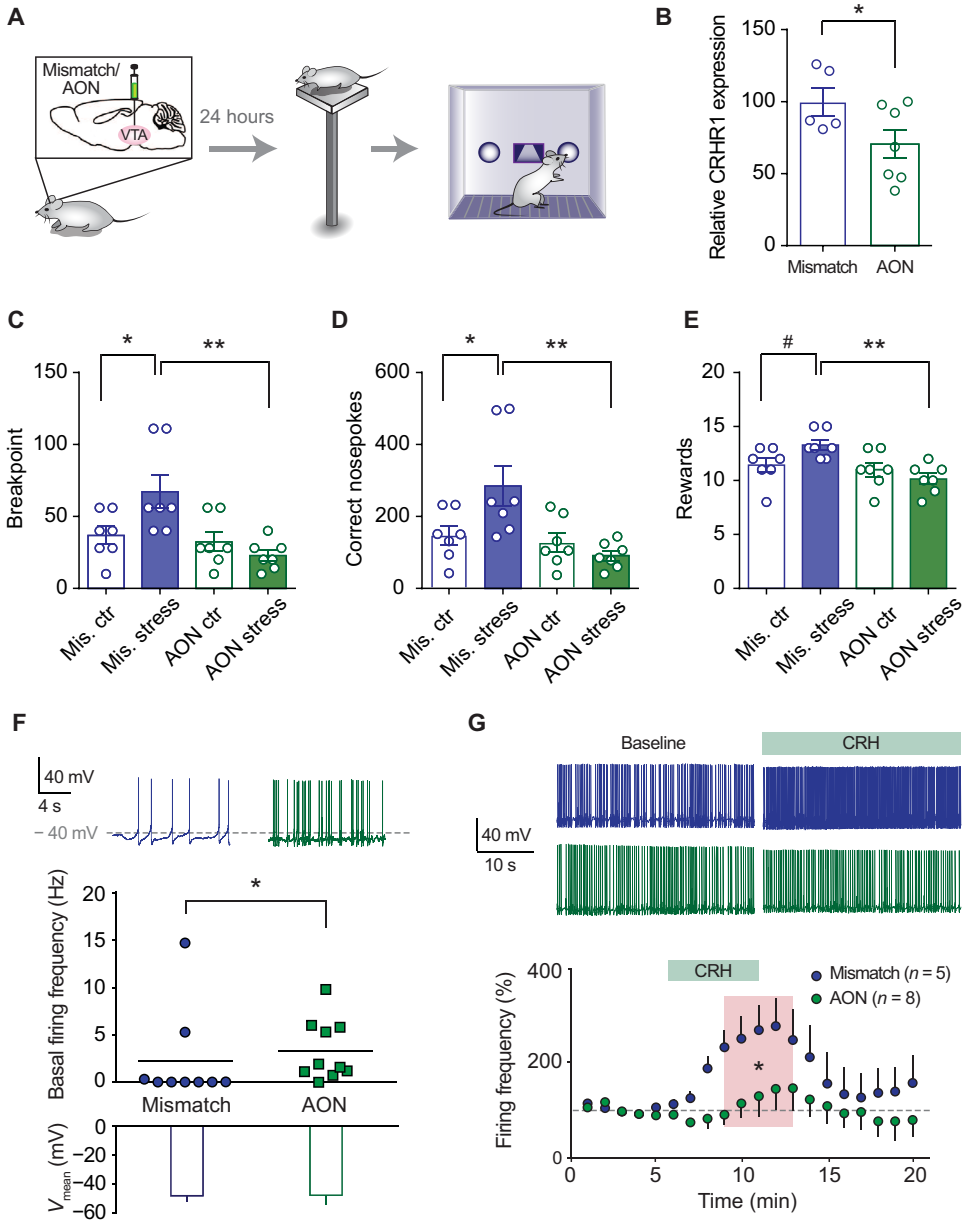

Fig. 5. Antisense-mediated CRHR1 down-regulation in the VTA blocks stress effects on PR performance in LA rats. (**A**) Schematic representation of AON treatment and PR test. (**B**) Treatment with AONs decreased CRHR1 expression in the VTA (one-tailed *t* test, $t_{11} = 2.199$, $P = 0.025$). (**C**) Significant AON treatment × stress interaction, significant treatment effect, and a nonsignificant effect of stress on breakpoint (two-way ANOVA: $F_{1,24} = 6.789$, $P = 0.016$, $F_{1,24} = 10.27$, $P = 0.004$, and $F_{1,24} = 1.872$, $P = 0.184$, respectively, $n = 7$). (**D**) Significant AON treatment effect, significant interaction, and nonsignificant effect of stress on the number of correct nosepokes (two-way ANOVA: $F_{1,24} = 9.566$, $P = 0.005$, $F_{1,24} = 6.346$, $P = 0.019$, and $F_{1,24} = 2.146$, $P = 0.156$, respectively, $n = 7$). (**E**) Two-way ANOVA revealed a significant AON treatment × stress interaction, a significant effect of AON treatment, and a nonsignificant effect of stress on the number of rewards ($F_{1,24} = 5.526$, $P = 0.027$, $F_{1,24} = 9.566$, $P = 0.005$, and $F_{1,24} = 0.75$, $P = 0.395$, respectively, $n = 7$). (**F**) Ex vivo basal firing rate of DA neurons in the VTA, following AON-mediated CRHR1 down-regulation. Treatment with AONs down-regulating CRHR1 resulted in a higher spontaneous firing rate in DA neurons compared to the mismatch treated group (Mann-Whitney test, $U = 17.5$, $P = 0.0222$, $n = 9$ to 10). (**G**) Bath application of CRH (500 nM) induced a reversible increase in cell firing in LA rats, which was partially blocked by AON treatment (Mann-Whitney test comparing mean values in the shaded area, $U = 6$, $P = 0.0451$, $n = 5$ to 8). Representative voltage traces are shown at the top. Asterisks denote significant differences in the respective post hoc tests (**$P < 0.01$, *$P < 0.05$, and $^{\#}P < 0.1$).

subsequently injected with AONs or mismatch (mis.) oligonucleotides for three consecutive days before PR test. The two groups did not differ in performance at training (fig. S4A). The expected stress-induced improvement in performance was verified in mismatch-treated LA rats but was prevented by AON treatment [two-way ANOVA revealed a significant AON treatment × stress interaction for breakpoint ($F_{1,24}$ = 6.789, P = 0.016; Fig. 5C), number of correct nosepokes performed ($F_{1,24}$ = 6.346, P = 0.019; Fig. 5D), and number of obtained rewards ($F_{1,24}$ = 5.526, P = 0.027; Fig. 5E)]. Stress-exposed mismatch-treated rats exhibited improved performance as compared to control rats and to stress-exposed rats treated with AONs targeting CRHR1. No effects of CRHR1-AON treatment or stress exposure were observed on the number of incorrect nosepokes (fig. S4B) during the PR test or in the number of correct nosepokes during the timeout period (fig. S4C).

To verify that the AON treatment effectively induced CRHR1 down-regulation in the VTA, and to examine the resulting changes in the DA neuron excitability and responsiveness to CRH, we conducted ex vivo patch clamp recordings from AON- and mismatch-treated rats. DA neurons from rats treated with AONs targeting CRHR1 exhibited higher rates of spontaneous firing (Fig. 5F), without further changes in basal cellular properties (fig. S4, D to I). Bath application of CRH (500 nM) induced a reversible increase in cell firing in DA neurons, which was significantly smaller in AON-treated rats than in mismatch-treated rats (Fig. 5G). Thus, AON-treated DA neurons from LA rats exhibit a CRH responsiveness that is comparable to DA neurons from HA rats.

CRHR1 overexpression in VTA → NAc projection neurons improves motivated behavior under stress

Next, we investigated whether overexpressing CRHR1 in the VTA in rats high in anxiety would be sufficient to improve their motivated behavior under stress. To this end, we applied an intersection approach to specifically target VTA → NAc projecting neurons. Specifically, we infused (i) an AAVrg-pgk-Cre virus with retrograde infection properties, expressing Cre recombinase in the NAc, and (ii) either a CRHR1-overexpression virus (pAAV-CBA-Stop-CRHR1-WPRE, CRHR1 OE rats) or a green fluorescent protein (GFP)–expressing virus (pAAV-Stop-GFP) as control (GFP rats) in the VTA (Fig. 6). RNAscope analyses in samples obtained 4 weeks after viral infusion indicated that ~85% of the neurons that expressed the virus were DA neurons, in line with previous studies that have shown that the majority of neurons that project from the VTA to the NAc are DA neurons (fig. S5, D and E) (*43*). Moreover, CRHR1 expression was higher in DA neurons expressing the CRHR1 OE virus than in those expressing GFP (fig. S5F). Then, in a separate group of animals,

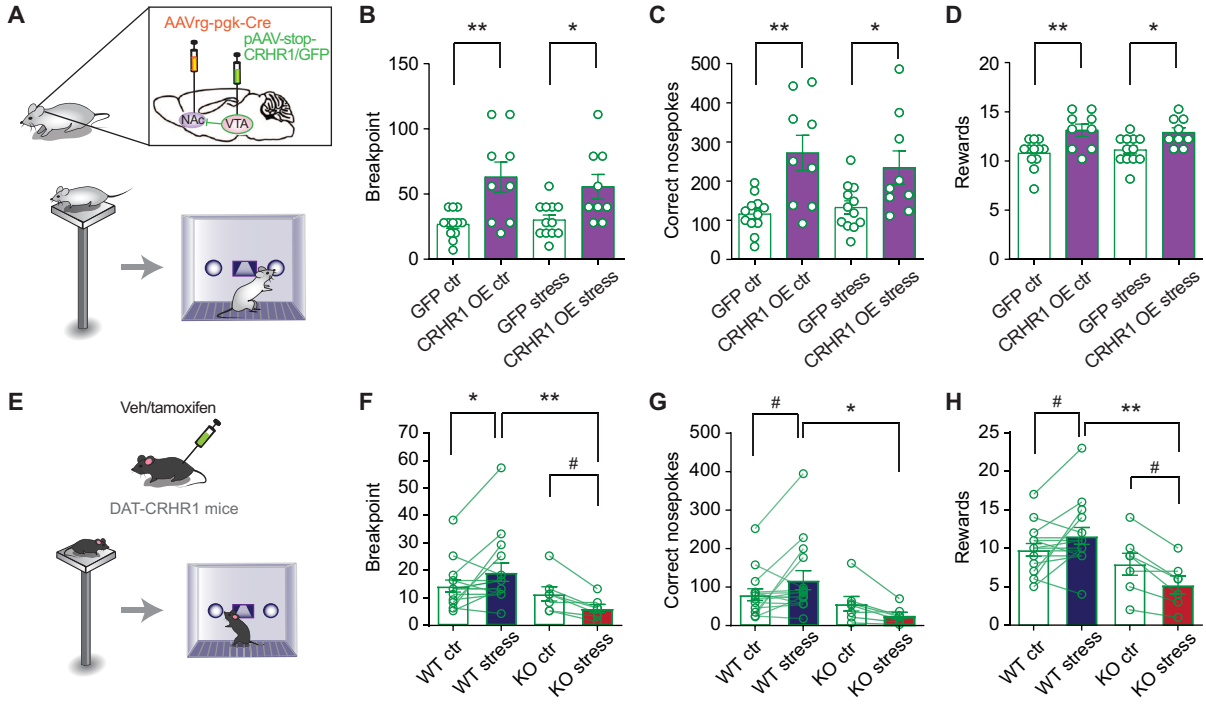

Fig. 6. Genetic manipulation of CRHR1 expression affects motivated behavior after stress. (**A**) Schematic representation of the viral strategy for CRHR1 OE or GFP expression in NAc-projecting VTA neurons in HA rats, generating CRHR1 OE rats and control GFP rats, which were tested for PR performance following stress exposure. (**B** to **D**) CRHR1 OE rats reached a higher breakpoint ($F_{1,19}$ = 12.43, P = 0.0027), performed more nosepokes ($F_{1,19}$ = 13.23, P = 0.0018), and obtained more rewards ($F_{1,19}$ = 12.06, P = 0.0025) both under basal conditions and after stress. (**E**) PR performance after stress was tested in DAT-CRHR1 mice in which CRHR1 was selectively down-regulated in DA neurons. (**F** to **H**) Stress in DAT-CRHR1 mice led to impaired performance. (F) Stress in DAT-CRHR1 mice led to a lower breakpoint. Two-way repeated-measures ANOVA revealed a significant stress × genotype interaction ($F_{1,20}$ = 8.028, P = 0.01), a marginally nonsignificant genotype effect, and a nonsignificant stress effect ($F_{1,20}$ = 4.016, P = 0.059 and $F_{1,20}$ = 0.004, P = 0.95, n = 7 to 15). (G) Stress reduced the number of correct nosepokes in DAT-CRHR1 mice. Two-way repeated-measures ANOVA revealed a significant stress × genotype interaction ($F_{1,20}$ = 5.836, P = 0.025), a marginally nonsignificant genotype effect, and a nonsignificant stress effect ($F_{1,20}$ = 4.013, P = 0.059 and $F_{1,20}$ = 0.056, P = 0.82, n = 7 to 15). (H) Stress in DAT-CRHR1 mice reduced reward acquisition. Two-way repeated-measures ANOVA revealed a significant stress × genotype interaction ($F_{1,20}$ = 10.14, P = 0.005), a significant effect of genotype, and a nonsignificant effect of stress ($F_{1,20}$ = 7.150, P = 0.014 and $F_{1,20}$ = 0.416, P = 0.53, n = 7 to 15 per group). Asterisks denote significant differences in the t test or post hoc test (**P < 0.01, *P < 0.05, and $^{\#}P$ < 0.1).

rats started training in an FR1 schedule 4 weeks after viral infusions. CRHR1 OE and GFP rats did not differ in their training performance (two-way repeated-measures ANOVA: interaction effect $F_{5,125} = 1.883$, $P = 0.101$, AON effect $F_{1,25} = 0.563$, $P = 0.46$, time effect $F_{5,125} = 51.35$, $P < 0.0001$; fig. S5A). However, CRHR1 OE rats showed superior performance than GFP rats when performing the PR test both under control conditions and under stress (breakpoint: Fig. 6B; number of correct nosepokes: Fig. 6C; and number of obtained rewards: Fig. 6D). There was no difference in the number of incorrect nosepokes performed during the PR test (fig. S5B), but CRHR1 OE rats performed more correct nosepokes in the timeout period (fig. S5C). The fact that CRHR1 OE rats already showed superior performance under basal conditions suggests that the surgery procedures may have reduced the threshold to display anxiety in this cohort of animals. Together, these data further support a role for CRHR1 in VTA → NAc projecting neurons in motivated performance.

CRHR1 deletion in DA neurons impairs motivated behavior under stress

AONs effectively down-regulated VTA responsiveness to CRH in rats but did not target CRHR1 in a cell type–specific manner. To investigate the effect of CRHR1 deregulation in DA neurons, we used DAT-CRHR1 mice, which is a tamoxifen-inducible model of CRHR1 deletion selectively in DA neurons and their Cre^- littermates (*41*). Following tamoxifen or vehicle treatment and habituation to the reversed light cycle, mice were trained in a FR1 schedule and were subsequently exposed to two progressive ratio test sessions on two consecutive days, first without exposure to stress (control) and then after a 15-min exposure to an EP (Fig. 6E). Our data show that, although there was no difference between WT and KO mice in the control progressive ratio test session, stress exposure resulted in a significantly better performance in WT mice compared to KO mice [breakpoint: two-way repeated-measures ANOVA revealed a significant stress × genotype interaction ($F_{1,20} = 8.028$, $P = 0.01$), Fig. 6F; correct nosepokes: two-way repeated-measures ANOVA revealed a significant stress × genotype interaction ($F_{1,20} = 5.836$, $P = 0.025$), Fig. 6G; rewards: two-way repeated-measures ANOVA revealed a significant stress × genotype interaction ($F_{1,20} = 10.14$, $P = 0.005$) and a significant effect of genotype ($F_{1,20} = 7.150$, $P = 0.014$), Fig. 6H]. For the comparison between WT and KO mice, we pooled Cre^- tamoxifen–treated, Cre^- vehicle–treated, and DAT-CRHR1 vehicle–treated mice as WT groups, after confirming lack of significant differences among them (fig. S6, B to D). When mice were given free access to sucrose pellets, there was no difference in consumption between WT and KO mice, with or without prior stress exposure (fig. S6E). Moreover, the number of inactive nosepokes was not different between genotypes or after stress exposure compared to control (fig. S6F). Last, there was no difference between WT and KO mice in training performance, suggesting that the CRHR1 KO in DA neurons did not have an effect in learning (fig. S6G).

DISCUSSION

In this study, we reveal divergent effects of acute stress in motivated behavior depending on individuals' anxiety and identify the CRH system in the VTA as a critical mediator of those distinct stress effects. Specifically, we show that acute stress exposure facilitates effort exertion to obtain rewards in LA rats, but it has the opposite—i.e., inhibitory—effect in effort exertion in HA rats, while not changing animals' interest to consume the rewards. We also underscore the crucial role for CRHR1 in the VTA in tuning the impact of stress both on the functioning of mesolimbic DA neurons and in the regulation of motivated behavior.

The existence of individual variation in the behavioral and cognitive effects of acute stress is being increasingly recognized (*13*–*18*), and its understanding is proving critical for progress in the field (*44*–*48*). However, it is unknown whether motivation is distinctly affected by acute stress in different individuals. Most reports to date have emphasized negative effects of acute stress in working for food rewards (*8*, *9*, *11*). Positive motivational qualities of acute stress have been barely recognized (*7*) and are much less understood (*49*). Most evidence on positive motivational effects of stress has been generated using pharmacological stressors and focusing on relapse to drugs of abuse (*50*) or on seeking for previously primed high-energy content food (*12*). In contrast to most studies in the field focusing on motivation for palatable food, in our study, we avoided restricting rats' access to food, which may create additional stress and, therefore, a different baseline. Here we show that acute exposure to natural stressors does not only dampen motivation as previously reported (*8*, *9*, *11*) but it can also invigorate work for primary rewards in a subset of individuals as it would be expected from the activating properties elicited by stress to facilitate survival (*1*, *2*, *49*). Acknowledging that acute stress exerts dichotomic effects in different individuals offers a more integrative view of the motivational impact of stress than the expectation of a homogeneous type of behavioral adaptation throughout the population. The understanding that under stress we are not all equal is in good agreement with the evolutionary view that the triggering of response variation by stress is a key mechanism of adaption (*51*).

Identifying trait anxiety as a critical phenotype moderating the motivational response to stress provides a useful tool to investigate the underlying mechanisms. The focus in the CRH system is grounded on its crucial role for the regulation of both stress and anxiety (*33*, *36*). Genetic variants in the *Crhr1* intron 1 region have been consistently associated with anxious behavior and gene × environment interactions in mice (*52*) and humans (*53*). In our study, we identified an SNP in intron 1 of *Crhr1* for which heterozygous rats are more likely to be LA than HA, indicating that heterozygosity in this SNP is associated with lower anxiety in Wistar rats. This intronic *Crhr1* variant breaks a CpG site located in a CpG island (*54*), likely determining differential DNA methylation profiles regulating gene expression. DNA methylation in the *Crhr1* gene has been related to anxiety disorders in humans (*55*). In addition, previous work implicated CRHR1 actions in the NAc in appetitive behaviors (*30*, *56*–*58*), while CRHR1 actions in the VTA in deleterious motivational effects of acute stress (*9*, *11*). Future research is warranted to investigate the effects of the identified SNP at the molecular level.

Our results here go well beyond those previous findings by identifying VTA CRHR1 as a key differential substrate for the opposite regulation of motivated behavior by a common stressful experience in individuals in the two sides of the anxiety spectrum. Specifically, by taking advantage of natural phenotypic variation in anxiety-like behaviors in outbred rats, we show that HA rats show lower CRHR1 expression in VTA DA, but not GABAergic, neurons than LA rats, possibly driven by genetic variations. These data are congruent with the increased anxiety observed in mice with genetic deletion of CRHR1 in DA, but not in GABAergic, neurons (*37*). Then, consistent with

the observed differences in VTA CRHR1 expression levels, CRH administration in the VTA mimicked stress effects in motivated behavior, leading to opposite outcomes in HA and LA rats. CRH also had a differential impact on VTA DA neuron firing frequency, triggering a marked increase from basal firing in LA animals while leading to a blunted responsiveness in HA rats. Although the effect of bath-applied CRH on VTA DA firing in our electrophysiological experiments was significantly different in the physiological submillimolar range (*33*), the dose-response curves for LA and HA rats appeared to converge at higher concentrations. This suggests that, in addition to a differential expression of the CRHR1, the agonist may also act with a different potency on CRHR1 in LA and HA rats to initiate the intracellular signaling leading to increased excitability.

The CRH-induced increase in VTA DA cell firing in LA rats relied on CRHR1—in agreement with previous findings (*59*)—but not on GABAergic activation. These differential changes in VTA DA cell firing were matched by greater DA levels in the NAc in LA than in HA rats following intra-VTA CRH injection. These results are in accordance with studies showing a correspondence between VTA DA neuron activity and DA release in the NAc (*60*–*62*) and align well with the DA decrease in the NAc observed upon reward delivery in demotivated animals injected with CRH into the VTA (*11*). Therefore, our data suggest that the higher VTA CRHR1 expression in LA rats enables DA neurons to steeply increase their firing upon stress and boost DA release in the NAc (*11*, *63*), which is critical for the proper orchestration of motivated behavior, including behavioral activation, exertion of effort, and energy expenditure (*64*, *65*). On the other hand, the blunted cellular effects of intra-VTA CRH may explain the impaired performance HA rats exhibited in the PR test following stress exposure and intra-VTA CRH treatment.

We provide evidence in support of this hypothesis through experiments that establish the causal involvement of VTA CRHR1 in the opposite pattern of performance under acute stress for rats at the two sides of the anxiety spectrum. Specifically, we show that (i) CRHR1 OE in VTA → NAc projecting neurons, the majority of which was DA neurons, in HA and IA rats enables better motivated performance and (ii) conversely, AON-induced CRHR1 down-regulation in the VTA in LA rats prevents both stress-induced facilitation of motivated behavior and CRH-induced increase in VTA DA neuron firing frequency. It should be noted that whereas the experiment involving AON-induced CRHR1 down-regulation in the VTA yielded no difference between control and stress on the breakpoint, DAT-CRHR1 mice showed a decrease in PR under stress. This difference is likely to be due to the different impact of the two knockdown approaches in both terms of cell specificity and extent of the DA neurons affected. The KO is restricted to DA neurons in DAT-CRHR1 mice, while the AON approach is not cell specific. In addition, the level of down-regulation of CRHR1 expression achieved through the AON strategy, while demonstrated in our study, is unlikely to be as exhaustive as the complete elimination of CRHR1 expression in DA neurons achieved through the Cre-recombinase system in DAT-CRHR1 mice. Last, we corroborate the involvement of CRHR1 in DA neurons in both stress-induced facilitation of motivated behavior and CRH increase of VTA DA neuronal firing frequency using mice lacking CRHR1 expression selectively in TH neurons. Current evidence indicates the existence of different opposing CRH-driven forces at play in the VTA: (i) direct actions on CRHR1 in DAergic cells resulting in an increase in DA neuron firing rate (*59*) and (ii) actions on VTA GABAergic neurons, ultimately leading to the inhibition of DA neuron firing (*40*). Hence, lower CRHR1 levels in VTA DA neurons reduce the possibility of increasing neuronal firing in response to CRH but may also allow higher susceptibility of VTA DA neurons to GABA-mediated inhibition (*40*) [which may be accompanied also by direct modulation of NAc neurons by GABAergic projections from the VTA (*66*)]. Together, our data establish that the levels of CRHR1 in VTA DA neurons—that vary with individuals' anxiety—act as a switching mechanism determining whether acute stress facilitates or dampens effortful motivation.

In addition, we find anxiety-dependent differences in the tonic firing of VTA DA neurons that may represent a further substrate to define stress susceptibility. Unlike in vivo, DA neurons in slices do not fire in bursts but display tonic pacemaking firing, due to lacking afferent control (*67*). The propensity of VTA → NAc projecting neurons to fire under basal conditions has emerged as a marker of vulnerability to chronic stress. Specifically, these neurons increase their tonic firing in slices from mice that developed depression-like behaviors following social defeat stress, but not in those resilient to stress (*68*–*70*). In addition, optogenetically induced phasic DA firing combined with a subthreshold chronic social defeat stress paradigm was sufficient to induce depression-like behaviors (*71*). Our ex vivo data indicating that higher levels of anxiety are associated with higher rates of spontaneous VTA DA firing regardless of stress exposure suggest that a priori susceptibility to stress may be reflected by differential firing properties in these neurons and may not only be the results of stress-induced adaptation. Our data also imply a key role for a differential expression of CRHR1 in these neurons in defining this latent susceptibility.

The fact that this latent susceptibility at the interface between CRHR1 and the VTA DA neurons is related to individuals' anxiety may be particularly relevant, given that high trait anxiety is emerging as a risk factor for the development of stress-related psychopathologies (*16*, *72*) that are often accompanied by motivational disturbances (*4*, *8*). Therefore, our findings reveal a differential latent predisposition to respond to motivational challenges under acute stress that is congruent with the higher vulnerability shown by HA individuals—as compared to LA ones—to develop passive coping behaviors when exposed to stressful challenges (*44*, *46*, *48*).

In conclusion, the present study reveals that acute stress affects motivational adaptations in opposite ways for individuals at the two sides of the anxiety spectrum, i.e., "invigorating" LA while "inhibiting" drive in HA individuals. This recognition of a differential sensitivity of individuals to exert incentivized effort under stress can help guide both personalized training and interventions to manage stress levels addressed to improve performance and productivity at work and educational settings. Furthermore, our study highlights CRHR1 in VTA DA neurons as a neurobiological substrate for anxiety-related motivational differences under stress, as both a biomarker and a potential target for therapeutic interventions.

MATERIALS AND METHODS

Animals

Rats

Adult male Wistar rats (Charles Rivers, Saint-German-Nuelle, France) weighing 250 to 275 g at the beginning of the experiment were used for all experiments. Rats were individually housed in cages in

housing colonies on a 12-hour/12-hour light-dark cycle with lights on at 7:00, apart from the rats used for operant conditioning experiments, which were placed in a reversed cycle (lights on at 20:00, lights off at 8:00). Food and water were available ad libitum. Following a week of acclimatization to the animal facilities, rats were handled for 2 min per day for 3 days before the start of the experiments to habituate to the experimenters. Sample sizes were calculated on the basis of previous experiments in our laboratory and similar experiments published in the literature. Within each anxiety subgroup, animals were randomly allocated to each experimental treatment or manipulation. Experiments were performed by experimenters blinded to anxiety phenotype or prior experimental manipulations.

Mice

For the selective KO of CRHR1 in midbrain DA neurons, DAT-CreERT2 × Crhr1floxed/floxed ($^{f/f}$) mice (DAT-CRHR1) were used (*41*). Mice were group-housed two to four per cage in housing colonies on a 12-hour/12-hour light-dark cycle with lights on at 7:00. For induction of the mutation, mice were treated with tamoxifen (50 mg/kg) (Baar, Switzerland) intraperitoneally or an equal volume of sunflower seed oil as control (Sigma-Aldrich, Darmstadt, Germany), once a day for five consecutive days, at least 4 weeks before behavioral experiments. Cre^{-} Crhr1$^{f/f}$ mice were treated similarly with tamoxifen or sunflower seed oil. Two weeks before the onset of operant conditioning training, mice were placed in a housing room where the day-night cycle was reversed (lights on at 20:00, lights off at 8:00) and stayed there until the end of the experiment. For analyses, Cre^{-} Crhr1$^{f/f}$ mice treated with tamoxifen or sunflower seed oil and DAT-CRHR1 mice treated with sunflower seed oil were grouped together as WT mice and compared to DAT-CRHR1 mice treated with tamoxifen (KO mice). Sample sizes were decided on the basis of previous experiments in our laboratory and genotype availability. Within each genotype, animals were randomly allocated to each treatment (tamoxifen or vehicle). Experiments were performed by experimenters blinded to prior treatment. All experiments were performed with the approval (authorization number: VD3126) of the Cantonal Veterinary Authorities (Vaud, Switzerland) and carried out in accordance with the European Communities Council Directive of 22 September 2010 (2010/63/EU).

Anxiety classification

All rats were first tested in the EPM test to determine anxiety-related behavior, as previously described (*24*). Briefly, the EPM consisted of two open and two closed arms (45 cm × 10 cm each) extending from a 10 cm × 10 cm central area. Closed arms had 10-cm-high walls. Lighting was maintained at 16 to 17 lx in the open arms, 10 to 11 lx in the central area, and 5 to 7 lx in the closed arms. Rats were placed on the central area, facing a closed arm, and were allowed to explore freely for 5 min. Every animal was recorded, and tracking was performed using EthoVision software (Noldus, Wageningen, The Netherlands). Depending on their performance, they were classified as LA (more than 20% of time spent in the open arms), IA (between 5 and 20% of time spent in the open arms), or HA (less than 5% of time spent in the open arms) (*24*).

Genotyping

Genomic DNA was extracted from rats' brain tissue (26 HA, 32 IA, and 35 LA) using the DNeasy Blood and Tissue Kit (Qiagen AG, Hombrechtikon, Switzerland) as per the manufacturer's instructions. We targeted region crh10: 92189373-92191965, using seven primer pairs (table S2). This genomic region includes the proximal *Crhr1* promoter, where polymorphisms have been previously described (*73*, *74*), as well as part of the first intron of the gene. For each PCR, 6 μl of repliQa HiFi ToughMix (Quanta Bio, Beverly, MA, USA) was used, together with 0.5 μl of forward and reverse primer, 4.5 μl of water, and 0.5 μl of DNA for each sample. PCR started with a denaturation step at 95°C for 10 min, followed by 40 cycles of 15 s at 95°C and 1 min at 68°C, with a final extension step at 68°C for 10 min. Subsequently, the seven PCR products of each sample were pooled together in a single tube and library preparation continued using the Nextera XT Kit for library tagging and amplification, as per the manufacturer's instructions. Subsequently, DNA libraries were purified using the Agencourt AMPure XP reagent (Beckman Coulter, Nyon, Switzerland), as per the manufacturer's instructions.

Sequencing was performed using the MiSeq Illumina system to generate a total of 25 million reads. Quality control of the raw sequencing data was performed with FastQC version 0.11.9 (*75*). Subsequent adapter trimming of the data was performed with bcl2fastq version 2.20.0. Minimal read length tolerated post-trimming was 35 base pairs (bp). The reads were aligned to the *Rattus norvegicus* reference genome rn6 using the STAR aligner with default parameters (GenBank assembly accession: GCA_000001895.4) (*76*). The BAM files produced by the STAR aligner were analyzed using the bcftools mpileup and call utilities to produce the variant calls (*77*) (10.5281/zenodo.5749998).

Stereotactic surgery

VTA cannulation–NAc microdialysis guide cannula implantation

Rats were anesthetized by isoflurane inhalation (4%, for 4 min) in an induction chamber and maintained afterward with 2% isoflurane with a flow of 4 liters/min. Stereotactic surgery was performed as previously described (*24*, *38*, *78*). Briefly, rats were mounted on a stereotactic frame (Kopf Instruments, Tujunga, CA, USA), an incision was made along the midline of the skull, the periosteum was removed, and small holes were drilled for the implantation of guide cannulae (Invivo1, Roanoke, VA, USA). Coordinates were taken from the Paxinos and Watson brain atlas, relative to bregma, as follows: anterior-posterior: −5.8, mediolateral: ±2.2, dorsoventral: −6.45. VTA guide cannulae were inserted at an angle of 11°. For microdialysis, a CMA 12 guide cannula (CMA Microdialysis AB, Kita, Sweden) was implanted unilaterally in the NAc in the following coordinates, relative to bregma: anterior-posterior: +1.2, mediolateral: −1.5, dorsoventral: −6.5. NAc guide cannulae were inserted at an angle of 0°. Cannulae were fixated on the skull with three anchoring screws and Paladur acrylic dental cement (Kulzer, Hanau, Germany). Correct cannula placement was confirmed in the end of experiments.

CRHR1 OE

To overexpress CRHR1 in the VTA neurons that project to the NAc, HA and IA rats were treated with a retrograde Cre recombinase (Cre)–expressing virus (AAVrg-pgk-Cre available from P. Aebischer, Addgene viral preparation no. 24593) in the NAc (anterior-posterior: +1.2, mediolateral: ±1.5, dorsoventral: −7.5). A total of 1 μl at a rate of 0.1 μl/min was infused. During the same surgery, rats were infused in the VTA (anterior-posterior: −5.8, mediolateral: ±0.7, dorsoventral: −8.45) with a Cre-inducible CRHR1-expressing adeno-associated virus (pAAV-CBA-Stop-CRHR1-WPRE, a generous gift from A. Hansson, T. Klügmann, and G. von Jonquieres) (*79*) or a

Cre-inducible GFP-expressing adeno-associated virus (pAAV pCAG-FLEX-EGFP-WPRE, a gift from H. Zeng, Addgene viral preparation no. 51502-AAV2), as control. A total of 1 μl at a rate of 0.1 μl/min was infused.

Stress exposure

For experiments involving exposure to stress, rats were placed on square EPs (20 cm × 20 cm, at a height of 95 cm) under intense light (600 lx) for 15 min, immediately before the beginning of the progressive ratio sessions. Mice were placed on smaller square elevated (10 cm × 10 cm, at a height of 95 cm) platforms under intense light (600 lx) for 15 min, immediately before the beginning of the progressive ratio sessions.

Corticosterone assays

For the assessment of corticosterone concentration in the plasma upon stress exposure, blood samples were collected at different time points at the offset of the EP exposure into ice-cold heparin-coated capillary tubes (Sarstedt, Switzerland) and chilled until centrifugation (10,000 rpm at 4°C for 4 min). The control group was composed of rats taken from their home cage. Plasma was collected into new tubes and stored at −20°C until subsequent analysis. Free corticosterone was measured in the plasma samples (dilution 1:20) using an enzymatic immunoassay kit, performed according to the manufacturer's instructions (Enzo Life Sciences, Switzerland). Levels were calculated using a standard curve method.

Drug infusions

Behavioral experiments were generally performed 30 min after CRH or vehicle administration. CRH (Bachem, Bubendorf, Switzerland) was dissolved in artificial cerebrospinal fluid (aCSF) at a concentration of 2 μg/μl. For local intracerebral infusions, the dummy cannulae were removed and injectors were inserted extending 2 mm from the guide cannulae. CRH or vehicle was bilaterally infused intra-VTA at a volume of 0.5 μl per hemisphere at a rate of 0.15 μl/min. The injector remained in place for one additional minute after infusion to allow proper diffusion.

Operant conditioning

At least 10 days after surgery or after introduction to the reversed light-dark cycle (15 days in mice), animals started training in an FR1 reinforcement schedule. Operant chambers (Coulbourn Instruments, Holliston, MA, USA), placed in sound attenuating cubicles, were equipped with a grid, underneath which a tray with standard bedding material was placed for collection of feces and urine after each training session. Each chamber had one food tray and two ports placed on either side of the tray. A cue light was placed in each port and the food tray, whereas a house light was placed above the food tray. The right-hand side port of each chamber was designated as "active," meaning that spontaneous nosepoking would result in the drop of one 45-mg (20 mg for mice) food pellet (Bio-Serv, Flemington, NJ, USA) to the food tray. Upon nosepoking in the active port, the cue and house lights turned off, while the tray light turned on and the pellet dropped to the food tray. The two ports remained inactive for 20 s, during which nosepokes would not result in the delivery of a new pellet (timeout period). Subsequently, the chamber returned to its initial condition. Each training session lasted maximally 2 hours or until a rat acquired 100 pellets (4 hours or 60 pellets, respectively, for mice). Each rat received six training sessions (one training on each day for five consecutive days, followed by 2 days without training and one more training session on day 8). Only rats that finished at least two training sessions acquiring 100 pellets before the 2-hour mark were used for progressive ratio reinforcement schedule (progressive ratio test) experiments. The criterion for mice was acquisition of >50% of the maximum possible number of pellets in at least two training sessions out of a total of seven training sessions.

To test motivated behavior, rats were exposed to a progressive ratio test. Progressive ratio test sessions were identical to training sessions except that the operant requirement in each trial (T) was the integer (rounded down) of the function $1.4^{(T-1)}$ starting at one nosepoke for the first three trials and increasing in subsequent trials for rats, as has been previously described (*11*). For mouse experiments, the operant requirement for each trial (T) was the integer of the function $[5e^{(T)*0.2}] - 5$, as has been described (*80*). Correct nosepokes (i.e., nosepokes in the active port and outside the timeout period, thus resulting in food delivery), number of obtained sucrose pellets (rewards), and the last ratio completed (breakpoint) were calculated to evaluate behavioral performance (*80*, *81*). Data from at least two batches of animals were pooled for the final analysis of each experiment.

Free pellet consumption

Approximately a week after the end of the progressive ratio test session, animals were put in cages similar to their home cage, but without bedding material (to facilitate detection of pellets), and were given access to 20 sucrose pellets, identical to the ones used for operant conditioning sessions, for 15 min. In the end of the 15-min period, the remaining pellets (if any) were counted. Before the beginning of the session, animals were treated similarly to the progressive ratio test sessions (e.g., stress exposure-control or vehicle-CRH intra-VTA administration).

Fluorescence in situ hybridization (RNAscope) and confocal microscopy

HA and LA rats were decapitated, and their brains were then harvested and snap-frozen in isopentane on dry ice. Brains were stored at −80°C. Coronal sections at a thickness of 16 μm containing the VTA were cut using a Leica CM cryostat at −20°C and mounted on Superfrost plus glass slides (Electron Microscopy Sciences, Hatfield, PA, USA). Slides were stored at −80°C until further processing. Fluorescence in situ hybridization was performed using RNAscope (Advanced Cell Diagnostics, Newark, CA, USA), as per the manufacturer's instructions (*82*). Briefly, slides were fixed in 10% neutral buffered formalin for 20 min at 4°C. Slides were washed 2 × 1 min with 1× phosphate-buffered saline (PBS), before dehydration with 50% ethanol (1 × 5 min), 70% ethanol (1 × 5 min), and 100% ethanol (2 × 5 min). Subsequently, slides were dried at room temperature (RT) for 10 min. A hydrophobic barrier was drawn around the sections using a hydrophobic pen and allowed to dry for 15 min at RT. Sections were then incubated with Protease Pretreat-4 solution for 20 min at RT. Slides were washed with ddH_2O (2 × 1 min), before being incubated with the appropriate probes for 2 hours at 40°C in the HybEZ oven. The following probes were purchased: Rn-*Crhr1*-C1 (catalog no. 318911), Rn-Gad1-C2 (catalog no. 316401), and Rn-TH-C3 (catalog no. 314651). Following incubation with the appropriate probes, slides were subjected to a series of amplification steps (Amp 1 at 40°C for 30 min, Amp 2 at 40°C for 30 min, and

Amp 3 at 40°C for 15 min). A DAPI-containing solution was applied to sections at RT for 20 s. Last, slides were coverslipped using ProLong Gold Antifade mounting media and stored at 4°C until imaging on a confocal microscope (LSM700, Zeiss, Feldbach, Switzerland). Confocal images were analyzed using a plugin for Fiji (*83*). The number of *Crhr1* puncta in the areas of colocalization of DAPI with TH or GAD1 was calculated in 6 to 12 images in two sections for each animal, and the result was presented as the number of dots/the total area of colocalization between DAPI and TH or DAPI and GAD1.

To study whether viral vectors were preferentially expressed in DA neurons, we used a similar protocol, targeting CRHR1 [Rn-*Crhr1*-C1 (catalog no. 318911)], TH [Rn-TH-C3 (catalog no. 314651)], and WPRE [Woodchuck Hepatitis Virus Posttranscriptional Regulatory Element WPRE-O1-C2 (catalog no. 450261-C2)], which was common for both GFP and CRHR1 OE virus and could only be expressed if cells were also expressing the retro-cre virus. Subsequently, we used QuPath to quantify the number of cells expressing the GFP or CRHR1 OE virus and how many of them were also DA neurons (TH^+), using 6 to 12 images per animal. Last, we quantified the expression of CRHR1 in the areas of the VTA in the images, where WPRE and TH expression was colocalized.

Immunofluorescence staining and confocal microscopy

Immunofluorescence analysis was performed as previously described (*38*). Briefly, rats were anesthetized with a lethal dose of pentobarbital (Esconarkon, Streuli Pharma, Uznach, Switzerland) and euthanized by transcardial perfusion using a 0.9% saline solution followed by perfusion with a solution of 4% paraformaldehyde (Electron Microscopy Sciences, Hatfield, PA, USA) in PBS (pH 7.5). The brains were harvested, postfixated overnight in 4% paraformaldehyde/PBS at 4°C, and cryoprotected in 30% sucrose/PBS. Coronal sections (30 μm thick) were cut on a CM3050 S cryostat (Leica, Wetzlar, Germany) and stored in antifreeze solution at −20°C, until further processing. Free-floating sections were triple labeled for CRHR1, DAPI, and TH. Free-floating sections were washed three times for 10 min with PBS, then blocked for 1 hour in PBS–0.1% Triton X-100 (Sigma-Aldrich, Darmstadt, Germany)–5% normal donkey serum (Jackson ImmunoResearch, Cambridge, UK), and incubated overnight at 4°C with rabbit anti-CRHR1 (NLS1778, Novus Biologicals, Littleton, CO, USA; 1:250) and chicken anti-TH (ab134461, Abcam, Cambridge, UK; 1:250). Subsequently, sections were washed three times for 10 min and then incubated for 2 hours at RT with the following secondary antibodies, as needed: donkey anti-rabbit conjugated with an Alexa Fluor 568 fluorophore (A10042, Invitrogen, Carlsbad, CA, USA; 1:1000) and goat anti-chicken conjugated with an Alexa Fluor 488 fluorophore (A-11039, Invitrogen; 1:1000). Last, sections were incubated at RT for 10 min in a DAPI/PBS solution (Invitrogen; 1:10,000) and finally rinsed and mounted with Fluoromount-G (Southern Biotech, Birmingham, AL, USA).

Images were captured with a confocal microscope (LSM700, Zeiss, Feldbach, Switzerland) using a 20× objective. For visualization purposes, representative specific sections were zoomed and enhanced in a linear manner for brightness and contrast using FIJI software. Quantification was performed on original, unenhanced images only. To quantify CRHR1 expression, the background of each channel was measured at three different random areas around the section and averaged together to generate a mean background for each channel. This mean background was then subtracted from each channel. The total positive area of TH immunoreactivity was calculated, and CRHR1 expression was presented as percentage of TH or positive pixels that were also positive for CRHR1 over the total number of TH-positive pixels, for each section. Sections were then averaged to provide one value per animal per cell type of interest. For validation of antisense-mediated down-regulation of CRHR1, the total number of pixels positive for the fluorophore of the AONs was used for calculations. For quantification, the percentage of CRHR1-positive pixels was calculated over the total number of pixels positive for CRHR1 or DAPI staining.

Microdialysis

Rats were habituated to a plexiglass bowl, in which microdialysis took place, for 3 days for 20 min each day, before the beginning of microdialysis sessions. On the day of testing, animals were connected to a microdialysis setup by means of a microdialysis probe (CMA 12 Elite 8+1 mm, CMA Microdialysis AB, Kita, Sweden) inserted into the brain through which freshly made and filtered aCSF was pumped (CMA 4004 microdialysis pump, CMA) at a flow of 2 μl/min. Samples (20 μl) were collected every 20 min for 2 hours in a cooled (4°C) fraction collector (Microbiotech, Stockholm, Sweden) in vials containing perchloric acid (Sigma-Aldrich) (0.1 M in the samples) to prevent neurotransmitter breakdown. After 2 hours, CRH or vehicle was bilaterally infused intra-VTA and for the following 80-min samples were collected to investigate treatment effects. The average of the last three measurements before treatment was calculated and used as baseline for every rat. Posttreatment neurotransmitter release data are presented as percent of baseline.

High-performance liquid chromatography

DA and its metabolite, the intraneuronal DOPAC, were assayed by high-performance liquid chromatography (HPLC) with electrochemical detection. NAc perfusates in 0.1 M perchloric acid (20 μl) were used for determination of DA and DOPAC using HPLC.

The chromatograph HTEC-500 (Eicom, Ireland) was equipped with the Eicompak SC-3ODS column (Eicom) for monoamine analysis. The mobile phase consisted of 0.1 M citrate-acetate buffer (pH 3.5), sodium octane sulfonate (220 mg/ml), EDTA-2Na (5 mg/liter), and 20% methanol. The flow rate was maintained at 400 μl/min. DA and DOPAC were quantified by peak area comparisons with standards run on the day of the analysis (Eicom Envision EPC-700 software) and normalized as percentage of baseline metabolite levels before the vehicle or CRH treatment.

Ex vivo electrophysiology

Animals were anesthetized with isoflurane and decapitated. The brain was quickly removed, and horizontal brain slices (200 μm thick) containing the midbrain were prepared using a vibrating tissue slicer (Campden Instruments, Loughborough, UK) in oxygenated (95% O_2/5% CO_2) ice-cold modified aCSF containing 105 mM sucrose, 65 mM NaCl, 25 mM $NaHCO_3$, 2.5 mM KCl, 1.25 mM NaH_2PO_4, 7 mM $MgCl_2$, 0.5 mM $CaCl_2$, 25 mM glucose, and 1.7 mM L(+)-ascorbic acid. Slices recovered for 1 hour at 35°C in standard aCSF containing 130 mM NaCl, 25 mM $NaHCO_3$, 2.5 mM KCl, 1.25 mM NaH_2PO_4, 1.2 mM $MgCl_2$, 2 mM $CaCl_2$, 18 mM glucose, and 1.7 mM L(+)-ascorbic acid and complemented with 2 mM sodium pyruvate and 3 mM myo-inositol. In the recording chamber, slices were superfused with oxygenated standard aCSF at nearly physiological temperature (30° to 32°C). Neurons in the VTA were patched in the whole-cell configuration with borosilicate glass

pipettes (TW150F-3, WPI, Worcester, USA) pulled with a DMZ-Zeitz puller (Zeitz-Instruments, Martinsried, Germany). Patch pipettes (2 to 4 megohms) were filled with 130 mM potassium gluconate, 10 mM KCl, 10 mM Hepes, 10 mM sodium phosphocreatine, 0.2 mM EGTA, 4 mM Mg–adenosine triphosphate, and 0.2 mM Na–guanosine triphosphate (290 to 300 mOsm, pH 7.2 to 7.3). Recorded neurons were considered as DA if they exhibited I_h current/sag in response to hyperpolarizing voltage/current steps, as well as a >3-mV hyperpolarization upon perfusion of the $GABA_BR$ agonist baclofen (1 μM) at the end of the recording (see fig. S3, A to C) (*84*). Spontaneous cell firing was monitored in >30-s long gap free current clamp recordings with no current injection within the first 5 min after establishment of the whole-cell condition. Input-output curves of evoked spiking were constructed by providing 2-s-long incremental somatic current injections, while the membrane potential was held at −60 mV. The effect of CRH (500 nM) on spontaneous neuronal firing was tested after 5 min of stable baseline recording. In cells that exhibited no spontaneous spikes, firing during baseline was promoted by small current injections (<50 pA) that were kept constant throughout the recording.

Membrane voltage values were not corrected for liquid junction potential. Data were acquired through a Digidata 1550A digitizer. Signals were amplified through a MultiClamp 700B amplifier (Molecular Devices, Sunnyvale, USA), sampled at 20 kHz, and filtered at 10 kHz using Clampex 10 (Molecular Devices). Clampfit 10 (Molecular Devices) was used for data analysis. Dose-response curves for CRH were fitted in GraphPad using the function Y = Bottom + (Top − Bottom)/(1 + 10^((LogEC50 − X)*HillSlope)), where Bottom and Top are the plateau minimal and maximal responses, respectively.

AON treatment

Guide cannulae were implanted in the VTA as described above. Antisense (AON, sequence: CTGCGGGCGCCGTCC) and mismatch (sequence: CTTCGGGTAACGACC) DNA oligonucleotides (Eurogentec, Liege, Belgium), previously validated (*85*) with a full phosphorothioate backbone, were bilaterally infused (1 μl at a concentration of 1 μg/μl) in the VTA once per day for 3 days before the progressive ratio test, with the last infusion performed approximately 24 hours before the progressive ratio test. For experiments validating CRHR1 down-regulation, both oligonucleotides were labeled with an Alexa Fluor 488 fluorophore (Eurogentec).

Quantification of CRHR1 expression in the VTA of rats treated with AONs targeting CRHR1 and in DAT-CRHR1 mice

Rats treated with AONs targeting *Crhr1* or mismatch oligonucleotides or rats treated with pAAV-stop-CRHR1 or pAAV-stop-GFP were euthanized by rapid decapitation, and the brain was flash-frozen in ice-cold isopentane and then stored at −80°C. The VTA was dissected by punching 200-μm-thick section on a cryostat. Total RNA was extracted with the RNAqueous-Micro Kit (Thermo Fisher Scientific, Waltham, MA, USA) including deoxyribonuclease treatment. RNA (200 ng per sample) was converted into complementary DNA (cDNA) using qScript cDNA SuperMix (Quant Biosciences, Beverly, MA, USA). For qPCR, PCRs were performed in triplicates of cDNA using Power SYBR Green PCR Master Mix (Applied Biosystems, Thermo Fisher Scientific). Quantification was performed on a QuantStudio 6 Flex real-time PCR system (Applied Biosystems). *Crhr1* expression was calculated using the Pfaffl method (*86*) and normalized against the geometric mean of the expression of g-actin, EEf1, and TATA-box binding protein (TBP). Primers were as follows: actin G1 (forward: 5′-TAGTTCATGTGGCTCGGTCA-3′; reverse: 5′-GCTGGGGACTGACTGACTTT-3′), EEF1A1 (forward: 5′-TGTGGTGGAATCGACAAAAG-3′; reverse: 5′-CCCAGGCATACTTGAAGGAG-3′), and TBP (forward: 5′-CCCACCAGCAGTTCAGTAGC-3′; reverse: 5′-CAATTCTGGGTTTGATCATTCTG-3′). Primers for *Crhr1* were 5′-TCCGCTACAACACGACAAAC-3′ (forward) and 5′-AGAATCTCCTGGCACTCAGAA-3′ (reverse). To quantify *Crhr1* expression in the VTA of DAT-CRHR1 mice and control littermates, a similar procedure was followed. CRHR1 expression was calculated using the Pfaffl method (*86*) and normalized against the geometric mean of the expression of β-actin and EEF1A1. Primers were as follows: β-*actin* (forward: 5′-AGAGGGAAATCGTGCGTGAC-3′; reverse: 5′-CAATAGTGATGACCTGGCCGT-3′), *Eef1a1* (forward: 5′-TCCACTTGGTCGCTTTGCT-3′; reverse: 5′-CTTCTTGTCCACAGCTTTGATGA-3′), and *Crhr1* (forward: 5′-TCCGCTACAACACCACAAAC-3′; reverse: 5′-AGAATCTCCTGGCACTCAGAA-3′).

Statistics

The choice of parametric or nonparametric tests was based on normal distribution of the data (D'Agostino-Pearson normality test). When two groups were compared, one- or two-tailed *t* test or Mann-Whitney test was applied, as appropriate. When the effect of more than one independent variable was analyzed, two- or three-way ANOVA was used, followed by post hoc tests, as appropriate (Holm-Sidak or Fisher's least significant difference post hoc test). Outliers were detected and excluded using Grubb's test. Statistical analyses were performed with Prism 6 (GraphPad Software Inc., San Diego, CA) or Statistical Package for the Social Sciences (SPSS) version 17 (SPSS Inc., Chicago, IL, USA). Detailed parameters from statistical tests are reported in figure legends and in table S1. Statistical significance was set at $\alpha < 0.05$.

SUPPLEMENTARY MATERIALS

Supplementary material for this article is available at https://science.org/doi/10.1126/sciadv.abj9019

View/request a protocol for this paper from *Bio-protocol*.

REFERENCES AND NOTES

1. S. M. Korte, J. M. Koolhaas, J. C. Wingfield, B. S. McEwen, The Darwinian concept of stress: Benefits of allostasis and costs of allostatic load and the trade-offs in health and disease. *Neurosci. Biobehav. Rev.* **29**, 3–38 (2005).
2. B. S. McEwen, H. Akil, Revisiting the stress concept: Implications for affective disorders. *J. Neurosci.* **40**, 12–21 (2020).
3. L. D. Crocker, W. Heller, S. L. Warren, A. J. O'Hare, Z. P. Infantolino, G. A. Miller, Relationships among cognition, emotion, and motivation: Implications for intervention and neuroplasticity in psychopathology. *Front. Hum. Neurosci.* **7**, 261 (2013).
4. M. T. Treadway, N. A. Bossaller, R. C. Shelton, D. H. Zald, Effort-based decision-making in major depressive disorder: A translational model of motivational anhedonia. *J. Abnorm. Psychol.* **121**, 553–558 (2012).
5. E. Pulcu, P. D. Trotter, E. J. Thomas, M. McFarquhar, G. Juhasz, B. J. Sahakian, J. F. W. Deakin, R. Zahn, I. M. Anderson, R. Elliott, Temporal discounting in major depressive disorder. *Psychol. Med.* **44**, 1825–1834 (2014).
6. D. A. Pizzagalli, Depression, stress, and anhedonia: Toward a synthesis and integrated model. *Annu. Rev. Clin. Psychol.* **10**, 393–423 (2014).
7. W. J. Bowers, E. Attias, Z. Amit, Stress enhances the response to reward reduction but not food-motivated responding. *Physiol. Behav.* **67**, 777–782 (1999).
8. N. Shafiei, M. Gray, V. Viau, S. B. Floresco, Acute stress induces selective alterations in cost/benefit decision-making. *Neuropsychopharmacology* **37**, 2194–2209 (2012).
9. C. A. Bryce, S. B. Floresco, Perturbations in effort-related decision-making driven by acute stress and corticotropin-releasing factor. *Neuropsychopharmacology* **41**, 2147–2159 (2016).
10. B. Wang, Y. Shaham, D. Zitzman, S. Azari, R. A. Wise, Z. B. You, Cocaine experience establishes control of midbrain glutamate and dopamine by corticotropin-releasing factor: A role in stress-induced relapse to drug seeking. *J. Neurosci.* **25**, 5389–5396 (2005).

11. M. J. Wanat, A. Bonci, P. E. M. Phillips, CRF acts in the midbrain to attenuate accumbens dopamine release to rewards but not their predictors. *Nat. Neurosci.* **16**, 383–385 (2013).
12. X. Liu, Enhanced motivation for food reward induced by stress and attenuation by corticotrophin-releasing factor receptor antagonism in rats: Implications for overeating and obesity. *Psychopharmacology* **232**, 2049–2060 (2015).
13. T. Plieger, M. Reuter, Stress & executive functioning: A review considering moderating factors. *Neurobiol. Learn. Mem.* **173**, 107254 (2020).
14. C. W. E. M. Quaedflieg, H. Stoffregen, I. Sebalo, T. Smeets, Stress-induced impairment in goal-directed instrumental behaviour is moderated by baseline working memory. *Neurobiol. Learn. Mem.* **158**, 42–49 (2019).
15. L. Wirz, M. Reuter, J. Wacker, A. Felten, L. Schwabe, A haplotype associated with enhanced mineralocorticoid receptor expression facilitates the stress-induced shift from "Cognitive" to "Habit" learning. *eNeuro* **4**, ENEURO.0359-0317.2017 (2017).
16. M. Weger, C. Sandi, High anxiety trait: A vulnerable phenotype for stress-induced depression. *Neurosci. Biobehav. Rev.* **87**, 27–37 (2018).
17. R. M. Sapolsky, Stress and the brain: Individual variability and the inverted-U. *Nat. Neurosci.* **18**, 1344–1346 (2015).
18. B. Salehi, M. I. Cordero, C. Sandi, Learning under stress: The inverted-U-shape function revisited. *Learn. Mem.* **17**, 522–530 (2010).
19. M. Luethi, B. Meier, C. Sandi, Stress effects on working memory, explicit memory, and implicit memory for neutral and emotional stimuli in healthy men. *Front. Behav. Neurosci.* **2**, 5 (2008).
20. C. Sandi, Stress and cognition. *WIREs Cogn. Sci.* **4**, 245–261 (2013).
21. G. Luksys, W. Gerstner, C. Sandi, Stress, genotype and norepinephrine in the prediction of mouse behavior using reinforcement learning. *Nat. Neurosci.* **12**, 1180–1186 (2009).
22. M. Cordero, C. Sandi, Stress amplifies memory for social hierarchy. *Front. Neurosci.* **1**, 175–184 (2007).
23. L. Goette, S. Bendahan, J. Thoresen, F. Hollis, C. Sandi, Stress pulls us apart: Anxiety leads to differences in competitive confidence under stress. *Psychoneuroendocrinology* **54**, 115–123 (2015).
24. F. Hollis, M. A. van der Kooij, O. Zanoletti, L. Lozano, C. Cantó, C. Sandi, Mitochondrial function in the brain links anxiety with social subordination. *Proc. Natl. Acad. Sci. U.S.A.* **112**, 15486–15491 (2015).
25. A. I. Herrero, C. Sandi, C. Venero, Individual differences in anxiety trait are related to spatial learning abilities and hippocampal expression of mineralocorticoid receptors. *Neurobiol. Learn. Mem.* **86**, 150–159 (2006).
26. J. C. Thoresen, R. Francelet, A. Coltekin, K. F. Richter, S. I. Fabrikant, C. Sandi, Not all anxious individuals get lost: Trait anxiety and mental rotation ability interact to explain performance in map-based route learning in men. *Neurobiol. Learn. Mem.* **132**, 1–8 (2016).
27. T. T. J. Chong, V. Bonnelle, M. Husain, in *Progress in Brain Research*, B. Studer, S. Knecht, Eds. (Elsevier, 2016), vol. 229, pp. 71–100.
28. J. Epstein, D. Silbersweig, The neuropsychiatric spectrum of motivational disorders. *J. Neuropsychiatr. Clin. Neurosci.* **27**, 7–18 (2015).
29. R. Kanfer, M. Frese, R. E. Johnson, Motivation related to work: A century of progress. *J. Appl. Psychol.* **102**, 338–355 (2017).
30. N. G. Hollon, L. M. Burgeno, P. E. M. Phillips, Stress effects on the neural substrates of motivated behavior. *Nat. Neurosci.* **18**, 1405–1412 (2015).
31. S. Lammel, B. K. Lim, R. C. Malenka, Reward and aversion in a heterogeneous midbrain dopamine system. *Neuropharmacology* **76**, 351–359 (2014).
32. J. D. Salamone, M. Correa, The mysterious motivational functions of mesolimbic dopamine. *Neuron* **76**, 470–485 (2012).
33. J. M. Deussing, A. Chen, The corticotropin-releasing factor family: Physiology of the stress response. *Physiol. Rev.* **98**, 2225–2286 (2018).
34. M. J. A. G. Henckens, J. M. Deussing, A. Chen, Region-specific roles of the corticotropin-releasing factor–urocortin system in stress. *Nat. Rev. Neurosci.* **17**, 636–651 (2016).
35. K. Van Pett, V. Viau, J. C. Bittencourt, R. K. Chan, H. Y. Li, C. Arias, G. S. Prins, M. Perrin, W. Vale, P. E. Sawchenko, Distribution of mRNAs encoding CRF receptors in brain and pituitary of rat and mouse. *J. Comp. Neurol.* **428**, 191–212 (2000).
36. E. B. Binder, C. B. Nemeroff, The CRF system, stress, depression and anxiety—Insights from human genetic studies. *Mol. Psychiatry* **15**, 574–588 (2010).
37. D. Refojo, M. Schweizer, C. Kuehne, S. Ehrenberg, C. Thoeringer, A. M. Vogl, N. Dedic, M. Schumacher, G. von Wolff, C. Avrabos, C. Touma, D. Engblom, G. Schütz, K. A. Nave, M. Eder, C. T. Wotjak, I. Sillaber, F. Holsboer, W. Wurst, J. M. Deussing, Glutamatergic and dopaminergic neurons mediate anxiogenic and anxiolytic effects of CRHR1. *Science* **333**, 1903–1907 (2011).
38. M. A. van der Kooij, F. Hollis, L. Lozano, I. Zalachoras, S. Abad, O. Zanoletti, J. Grosse, I. G. de Suduiraut, C. Canto, C. Sandi, Diazepam actions in the VTA enhance social dominance and mitochondrial function in the nucleus accumbens by activation of dopamine D1 receptors. *Mol. Psychiatry* **23**, 569–578 (2018).
39. L. A. Sombers, M. Beyene, R. M. Carelli, R. Mark Wightman, Synaptic overflow of dopamine in the nucleus accumbens arises from neuronal activity in the ventral tegmental area. *J. Neurosci.* **29**, 1735–1742 (2009).
40. B. A. Harlan, H. C. Becker, J. J. Woodward, A. C. Riegel, Opposing actions of CRF-R1 and CB1 receptors on VTA-GABAergic plasticity following chronic exposure to ethanol. *Neuropsychopharmacology* **43**, 2064–2074 (2018).
41. R. E. Bernardi, L. Broccoli, N. Hirth, N. J. Justice, J. M. Deussing, A. C. Hansson, R. Spanagel, Dissociable role of corticotropin releasing hormone receptor subtype 1 on dopaminergic and D1 dopaminoceptive neurons in cocaine seeking behavior. *Front. Behav. Neurosci.* **11**, 221 (2017).
42. G. Liebsch, R. Landgraf, R. Gerstberger, J. C. Probst, C. T. Wotjak, M. Engelmann, F. Holsboer, A. Montkowski, Chronic infusion of a CRH1 receptor antisense oligodeoxynucleotide into the central nucleus of the amygdala reduced anxiety-related behavior in socially defeated rats. *Regul. Pept.* **59**, 229–239 (1995).
43. J. M. Breton, A. R. Charbit, B. J. Snyder, P. T. K. Fong, E. V. Dias, P. Himmels, H. Lock, E. B. Margolis, Relative contributions and mapping of ventral tegmental area dopamine and GABA neurons by projection target in the rat. *J. Comp. Neurol.* **527**, 916–941 (2019).
44. J. E. Castro, S. Diessler, E. Varea, C. Márquez, M. H. Larsen, M. I. Cordero, C. Sandi, Personality traits in rats predict vulnerability and resilience to developing stress-induced depression-like behaviors, HPA axis hyper-reactivity and brain changes in pERK1/2 activity. *Psychoneuroendocrinology* **37**, 1209–1223 (2012).
45. A. Cherix, T. Larrieu, J. Grosse, J. Rodrigues, B. McEwen, C. Nasca, R. Gruetter, C. Sandi, Metabolic signature in nucleus accumbens for anti-depressant-like effects of acetyl-L-carnitine. *eLife* **9**, e50631 (2020).
46. T. Larrieu, A. Cherix, A. Duque, J. Rodrigues, H. Lei, R. Gruetter, C. Sandi, Hierarchical status predicts behavioral vulnerability and nucleus accumbens metabolic profile following chronic social defeat stress. *Curr. Biol.* **27**, 2202–2210.e4 (2017).
47. J. Muir, Y. C. Tse, E. S. Iyer, J. Biris, V. Cvetkovska, J. Lopez, R. C. Bagot, Ventral hippocampal afferents to nucleus accumbens encode both latent vulnerability and stress-induced susceptibility. *Biol. Psychiatry* **88**, 843–854 (2020).
48. C. Nasca, C. Menard, G. Hodes, B. Bigio, C. Pena, Z. Lorsch, D. Zelli, A. Ferris, V. Kana, I. Purushothaman, J. Dobbin, M. Nassim, P. DeAngelis, M. Merad, N. Rasgon, M. Meaney, E. J. Nestler, B. S. McEwen, S. J. Russo, Multidimensional predictors of susceptibility and resilience to social defeat stress. *Biol. Psychiatry* **86**, 483–491 (2019).
49. J. C. Lemos, V. A. Alvarez, The upside of stress: A mechanism for the positive motivational role of corticotropin releasing factor. *Neuropsychopharmacology* **45**, 219–220 (2020).
50. S. G. Nair, T. Adams-Deutsch, D. H. Epstein, Y. Shaham, The neuropharmacology of relapse to food seeking: Methodology, main findings, and comparison with relapse to drug seeking. *Prog. Neurobiol.* **89**, 18–45 (2009).
51. A. A. Hoffmann, M. J. Hercus, Environmental stress as an evolutionary force. *Bioscience* **50**, 217–226 (2000).
52. C. Labermaier, C. Kohl, J. Hartmann, C. Devigny, A. Altmann, P. Weber, J. Arloth, C. Quast, K. V. Wagner, S. H. Scharf, L. Czibere, R. Widner-Andrä, J. Brenndörfer, R. Landgraf, F. Hausch, K. A. Jones, M. B. Müller, M. Uhr, F. Holsboer, E. B. Binder, M. V. Schmidt, A polymorphism in the Crhr1 gene determines stress vulnerability in male mice. *Endocrinology* **155**, 2500–2510 (2014).
53. P. B. Mahon, P. P. Zandi, J. B. Potash, G. Nestadt, G. S. Wand, Genetic association of FKBP5 and CRHR1 with cortisol response to acute psychosocial stress in healthy adults. *Psychopharmacology* **227**, 231–241 (2013).
54. R. Buels, E. Yao, C. M. Diesh, R. D. Hayes, M. Munoz-Torres, G. Helt, D. M. Goodstein, C. G. Elsik, S. E. Lewis, L. Stein, I. H. Holmes, JBrowse: A dynamic web platform for genome visualization and analysis. *Genome Biol.* **17**, 66 (2016).
55. C. Schartner, C. Ziegler, M. A. Schiele, L. Kollert, H. Weber, P. Zwanzger, V. Arolt, P. Pauli, J. Deckert, A. Reif, K. Domschke, CRHR1 promoter hypomethylation: An epigenetic readout of panic disorder? *Eur. Neuropsychopharmacol.* **27**, 360–371 (2017).
56. S. Peciña, J. Schulkin, K. C. Berridge, Nucleus accumbens corticotropin-releasing factor increases cue-triggered motivation for sucrose reward: Paradoxical positive incentive effects in stress? *BMC Biol.* **4**, 8 (2006).
57. J. C. Lemos, M. J. Wanat, J. S. Smith, B. A. S. Reyes, N. G. Hollon, E. J. van Bockstaele, C. Chavkin, P. E. M. Phillips, Severe stress switches CRF action in the nucleus accumbens from appetitive to aversive. *Nature* **490**, 402–406 (2012).
58. S. Hupalo, C. A. Bryce, D. A. Bangasser, C. W. Berridge, R. J. Valentino, S. B. Floresco, Corticotropin-releasing factor (CRF) circuit modulation of cognition and motivation. *Neurosci. Biobehav. Rev.* **103**, 50–59 (2019).
59. M. J. Wanat, F. W. Hopf, G. D. Stuber, P. E. M. Phillips, A. Bonci, Corticotropin-releasing factor increases mouse ventral tegmental area dopamine neuron firing through a protein kinase C-dependent enhancement of I_h. *J. Physiol.* **586**, 2157–2170 (2008).
60. S. Lohani, A. K. Martig, S. M. Underhill, A. DeFrancesco, M. J. Roberts, L. Rinaman, S. Amara, B. Moghaddam, Burst activation of dopamine neurons produces prolonged post-burst availability of actively released dopamine. *Neuropsychopharmacology* **43**, 2083–2092 (2018).

61. H.-C. Tsai, F. Zhang, A. Adamantidis, G. D. Stuber, A. Bonci, L. de Lecea, K. Deisseroth, Phasic firing in dopaminergic neurons is sufficient for behavioral conditioning. *Science* **324**, 1080–1084 (2009).
62. J. E. McCutcheon, J. J. Cone, C. G. Sinon, S. M. Fortin, P. A. Kantak, I. B. Witten, K. Deisseroth, G. D. Stuber, M. F. Roitman, Optical suppression of drug-evoked phasic dopamine release. *Front. Neural Circ.* **8**, 114 (2014).
63. L. S. Hwa, E. N. Holly, J. F. De Bold, K. A. Miczek, Social stress-escalated intermittent alcohol drinking: Modulation by CRF-R1 in the ventral tegmental area and accumbal dopamine in mice. *Psychopharmacology* **233**, 681–690 (2016).
64. J. D. Salamone, M. Pardo, S. E. Yohn, L. López-Cruz, N. S. Miguel, M. Correa, Mesolimbic dopamine and the regulation of motivated behavior. *Curr. Top. Behav. Neurosci.* **27**, 231–257 (2015).
65. J. D. Salamone, R. E. Steinpreis, L. D. McCullough, P. Smith, D. Grebel, K. Mahan, Haloperidol and nucleus accumbens dopamine depletion suppress lever pressing for food but increase free food consumption in a novel food choice procedure. *Psychopharmacology* **104**, 515–521 (1991).
66. D. C. Lowes, L. A. Chamberlin, L. N. Kretsge, E. S. Holt, A. I. Abbas, A. J. Park, L. Yusufova, Z. H. Bretton, A. Firdous, A. G. Enikolopov, J. A. Gordon, A. Z. Harris, Ventral tegmental area GABA neurons mediate stress-induced blunted reward-seeking in mice. *Nat. Commun.* **12**, 3539 (2021).
67. A. A. Grace, Dysregulation of the dopamine system in the pathophysiology of schizophrenia and depression. *Nat. Rev. Neurosci.* **17**, 524–532 (2016).
68. D. Payer, B. Williams, E. Mansouri, S. Stevanovski, S. Nakajima, B. le Foll, S. Kish, S. Houle, R. Mizrahi, S. R. George, T. P. George, I. Boileau, Corticotropin-releasing hormone and dopamine release in healthy individuals. *Psychoneuroendocrinology* **76**, 192–196 (2017).
69. M. E. Fox, M. K. Lobo, The molecular and cellular mechanisms of depression: A focus on reward circuitry. *Mol. Psychiatry* **24**, 1798–1815 (2019).
70. J.-L. Cao, H. E. Covington, A. K. Friedman, M. B. Wilkinson, J. J. Walsh, D. C. Cooper, E. J. Nestler, M. H. Han, Mesolimbic dopamine neurons in the brain reward circuit mediate susceptibility to social defeat and antidepressant action. *J. Neurosci.* **30**, 16453–16458 (2010).
71. J. J. Walsh, A. K. Friedman, H. Sun, E. A. Heller, S. M. Ku, B. Juarez, V. L. Burnham, M. S. Mazei-Robison, D. Ferguson, S. A. Golden, J. W. Koo, D. Chaudhury, D. J. Christoffel, L. Pomeranz, J. M. Friedman, S. J. Russo, E. J. Nestler, M.-H. Han, Stress and CRF gate neural activation of BDNF in the mesolimbic reward pathway. *Nat. Neurosci.* **17**, 27–29 (2014).
72. C. Sandi, G. Richter-Levin, From high anxiety trait to depression: A neurocognitive hypothesis. *Trends Neurosci.* **32**, 312–320 (2009).
73. M. L. Logrip, J. R. Walker, L. O. Ayanwuyi, V. Sabino, R. Ciccocioppo, G. F. Koob, E. P. Zorrilla, Evaluation of alcohol preference and drinking in msP rats bearing a Crhr1 promoter polymorphism. *Front. Psychol.* **9**, 28 (2018).
74. A. C. Hansson, A. Cippitelli, W. H. Sommer, A. Fedeli, K. Bjork, L. Soverchia, A. Terasmaa, M. Massi, M. Heilig, R. Ciccocioppo, Variation at the rat Crhr1 locus and sensitivity to relapse into alcohol seeking induced by environmental stress. *Proc. Natl. Acad. Sci. U.S.A.* **103**, 15236–15241 (2006).
75. S. Andrews, FastQC: A quality control tool for high throughput sequence data (2010); www.bioinformatics.babraham.ac.uk/projects/fastqc/.
76. A. Dobin, C. A. Davis, F. Schlesinger, J. Drenkow, C. Zaleski, S. Jha, P. Batut, M. Chaisson, T. R. Gingeras, STAR: Ultrafast universal RNA-seq aligner. *Bioinformatics* **29**, 15–21 (2013).
77. H. Li, A statistical framework for SNP calling, mutation discovery, association mapping and population genetical parameter estimation from sequencing data. *Bioinformatics* **27**, 2987–2993 (2011).
78. M. A. van der Kooij, I. Zalachoras, C. Sandi, GABAA receptors in the ventral tegmental area control the outcome of a social competition in rats. *Neuropharmacology* **138**, 275–281 (2018).
79. L. Broccoli, S. Uhrig, G. von Jonquieres, K. Schönig, D. Bartsch, N. J. Justice, R. Spanagel, W. H. Sommer, M. Klugmann, A. C. Hansson, Targeted overexpression of CRH receptor subtype 1 in central amygdala neurons: Effect on alcohol-seeking behavior. *Psychopharmacology* **235**, 1821–1833 (2018).
80. N. R. Richardson, D. C. S. Roberts, Progressive ratio schedules in drug self-administration studies in rats: A method to evaluate reinforcing efficacy. *J. Neurosci. Methods* **66**, 1–11 (1996).
81. C. Soares-Cunha, B. Coimbra, A. David-Pereira, S. Borges, L. Pinto, P. Costa, N. Sousa, A. J. Rodrigues, Activation of D2 dopamine receptor-expressing neurons in the nucleus accumbens increases motivation. *Nat. Commun.* **7**, 11829 (2016).
82. J. C. Lemos, J. H. Shin, V. A. Alvarez, Striatal cholinergic interneurons are a novel target of corticotropin releasing factor. *J. Neurosci.* **39**, 5647–5661 (2019).
83. J. Schindelin, I. Arganda-Carreras, E. Frise, V. Kaynig, M. Longair, T. Pietzsch, S. Preibisch, C. Rueden, S. Saalfeld, B. Schmid, J. Y. Tinevez, D. J. White, V. Hartenstein, K. Eliceiri, P. Tomancak, A. Cardona, Fiji: An open-source platform for biological-image analysis. *Nat. Methods* **9**, 676–682 (2012).
84. E. B. Margolis, B. Toy, P. Himmels, M. Morales, H. L. Fields, Identification of rat ventral tegmental area GABAergic neurons. *PLOS ONE* **7**, e42365 (2012).
85. T. Skutella, J. C. Probst, U. Renner, F. Holsboer, C. Behl, Corticotropin-releasing hormone receptor (type I) antisense targeting reduces anxiety. *Neuroscience* **85**, 795–805 (1998).
86. M. Pfaffl, A new mathematical model for relative quantification in real-time RT-PCR. *Nucleic Acids Res.* **29**, e45 (2001).

Acknowledgments: We would like to thank A. C. Hansson, M. Klugmann, and G. Von Jonquieres for the gift of the CRHR1 overexpression plasmid. We thank B. Schneider for the packaging and production of the CRHR1 overexpression virus. We would like to thank N. Meyer, S. Montamat, A. Montant, and C. Yildirim for excellent assistance with immunofluorescence stainings. **Funding:** This work was supported by grants from the Swiss National Science Foundation (fund nos. 152614 and 176206) and intramural funding from the EPFL to C.S. I.Z. was supported by an EMBO long-term fellowship (ALTF 1537-2015), cofunded by Marie Curie actions (LTFCOFUND2013, GA-2013-609409). M.M. was supported by an internal grant from the Donders Centre for Medical Neurosciences of the Radboud University Medical Center and a personal travel grant from FENS. **Author contributions:** Concept development and experimental design: C.S., I.Z., and S.A. Animal surgeries: I.Z., J.G., and I.G.d.S. Behavioral tests and analyses: I.Z., J.G., and I.G.d.S. Ex vivo analyses: I.Z. and O.Z. Electrophysiological recordings and analyses: S.A. Analysis of the sequencing data: M.M. Provision of key resources: J.M.D. Writing: C.S., I.Z., and S.A. **Competing interests:** The authors declare that they have no competing interests. **Data and materials availability:** All data needed to evaluate the conclusions in the paper are present in the paper and/or the Supplementary Materials.

Submitted 9 June 2021
Accepted 31 January 2022
Published 23 March 2022
10.1126/sciadv.abj9019

ScienceAdvances

Opposite effects of stress on effortful motivation in high and low anxiety are mediated by CRHR1 in the VTA

Ioannis ZalachorasSimone AstoriMandy MeijerJocelyn GrosseOlivia ZanolettiIsabelle Guillot de SuduirautJan M. DeussingCarmen Sandi

Sci. Adv., 8 (12), eabj9019. • DOI: 10.1126/sciadv.abj9019

Science Advances (ISSN) is published by the American Association for the Advancement of Science. 1200 New York Avenue NW, Washington, DC 20005. The title *Science Advances* is a registered trademark of AAAS.